AEDC-TR-81-10

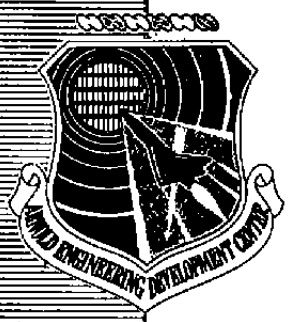

AEDC High-Enthalpy Ablation Test (HEAT) Facility Description, Development, and Calibration

D. D. Horn and R. T. Smith
ARO, Inc.

July 1981

Final Report for Period June 18, 1976 – September 30, 1977

Approved for public release, distribution unlimited

ARNOLD ENGINEERING DEVELOPMENT CENTER
ARNOLD AIR FORCE STATION, TENNESSEE
AIR FORCE SYSTEMS COMMAND
UNITED STATES AIR FORCE

NOTICES

When U. S. Government drawings, specifications, or other data are used for any purpose other than a definitely related Government procurement operation, the Government thereby incurs no responsibility nor any obligation whatsoever, and the fact that the Government may have formulated, furnished, or in any way supplied the said drawings, specifications, or other data, is not to be regarded by implication or otherwise, or in any manner licensing the holder or any other person or corporation, or conveying any rights or permission to manufacture, use, or sell any patented invention that may in any way be related thereto.

Qualified users may obtain copies of this report from the Defense Technical Information Center.

References to named commercial products in this report are not to be considered in any sense as an indorsement of the product by the United States Air Force or the Government.

This report has been reviewed by the Office of Public Affairs (PA) and is releasable to the National Technical Information Service (NTIS). At NTIS, it will be available to the general public, including foreign nations.

APPROVAL STATEMENT

This report has been reviewed and approved.

ROSS G. ROEPKE
Directorate of Technology
Deputy for Operations

Approved for publication:

FOR THE COMMANDER

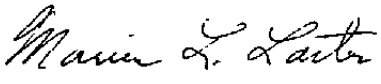

MARION L. LASTER
Director of Technology
Deputy for Operations

REPORT DOCUMENTATION PAGE		READ INSTRUCTIONS BEFORE COMPLETING FORM
1. REPORT NUMBER AEDC-TR-81-10	2. GOVT ACCESSION NO.	3. RECIPIENT'S CATALOG NUMBER
4. TITLE *(and Subtitle)* AEDC HIGH-ENTHALPY ABLATION TEST (HEAT) FACILITY DESCRIPTION, DEVELOPMENT, AND CALIBRATION		5. TYPE OF REPORT & PERIOD COVERED Final Report - June 18, 1976 - September 30, 1977 6. PERFORMING ORG. REPORT NUMBER
7. AUTHOR(s) D. D. Horn and R. T. Smith, ARO, Inc., AEDC Group, a Sverdrup Corporation Company		8. CONTRACT OR GRANT NUMBER(s)
9. PERFORMING ORGANIZATION NAME AND ADDRESS Arnold Engineering Development Center/DOT Air Force Systems Command Arnold Air Force Station, TN 37389		10. PROGRAM ELEMENT, PROJECT, TASK AREA & WORK UNIT NUMBERS Program Element 65807F
11. CONTROLLING OFFICE NAME AND ADDRESS Arnold Engineering Development Center/DOS Air Force Systems Command Arnold Air Force Station, TN 37389		12. REPORT DATE July 1981 13. NUMBER OF PAGES 65
14. MONITORING AGENCY NAME & ADDRESS *(if different from Controlling Office)*		15. SECURITY CLASS. *(of this report)* UNCLASSIFIED 15a. DECLASSIFICATION DOWNGRADING SCHEDULE N/A

16. DISTRIBUTION STATEMENT *(of this Report)*

Approved for public release; distribution unlimited.

17. DISTRIBUTION STATEMENT *(of the abstract entered in Block 20, if different from Report)*

18. SUPPLEMENTARY NOTES

Available in Defense Technical Information Center (DTIC).

19. KEY WORDS *(Continue on reverse side if necessary and identify by block number)*

arc heaters	heat transfer
test facilities	enthalpy
ablation	reentry vehicles
erosion	heat resistant materials

20. ABSTRACT *(Continue on reverse side if necessary and identify by block number)*

The Arnold Engineering Development Center (AEDC) has finished installation of a new ablation test unit which utilizes a high-performance segmented arc heater. This report describes the facility, the preliminary performance of the arc heater, and representative flow calibration measurements made with the arc heater operating at air pressures up to 124 atm. The results show that the arc heater is a reliable hot gas source capable of supplying the extremely hostile environment required for testing ablation specimens.

DD FORM 1 JAN 73 1473 EDITION OF 1 NOV 65 IS OBSOLETE

AFSC
Arnold AFS Tenn

PREFACE

The work reported herein was conducted by the Arnold Engineering Development Center (AEDC), Air Force Systems Command (AFSC). The results were obtained by ARO, Inc., AEDC Group (a Sverdrup Corporation Company), operating contractor for the propulsion test facilities at AEDC, AFSC, Arnold Air Force Station, Tennessee, under ARO Projects No. P32S-E2A and P32S-L9A. The Air Force project manager was Marshall Kingery, DOT.

CONTENTS

ILLUSTRATIONS

Figure

TABLES

1.0 INTRODUCTION

1.1 JUSTIFICATION

Reentry vehicles (RV) for ballistic missile systems commonly employ a covering of ablative material for heat protection. The nosetip of the vehicle, normally a spherically blunted cone, is subjected to a much higher heating rate than the rest of the vehicle and the heating rate increases with increasing reentry velocity. There is a continuing effort to develop better materials for nosetips, and ground test facilities are required to evaluate the performance of these materials in a timely and economical manner. Unfortunately, the test conditions required to simulate flight environments have continuously outpaced the performance capability of ground test facilities. No existing continuous flow facility can duplicate simultaneously the enthalpies and pressures encountered in flight by current reentry vehicles, and the discrepancy is even greater for the vehicles under development.

1.2 HISTORY OF ARCS AT AEDC

Arc-heated test facilities were first operated at the Arnold Engineering Development Center (AEDC) in 1962 with the objective of investigating nozzle throat cooling techniques applicable to tests requiring correct simulation of the free-stream temperature.

The original arc heater, a Huels type obtained from the Linde Company, operated at a chamber pressure of 73 atm and an energy balance enthalpy of 2,700 Btu/lb (Ref. 1). The heater was later modified and the operating conditions increased to 100-atm pressure and 2,500-Btu/lb enthalpy. In mid-1966, the heater was combined with a multiple-position model injection system to permit ablation testing of RV nosetips and heat shields (Ref. 2). Continuous studies and investigations have been conducted at AEDC to improve arc heater performance and thereby the testing capabilities of the ablation facilities.

In 1967, the AEDC contracted with Electro-Optical Systems, Inc., to develop a high-pressure, high-enthalpy segmented arc heater (Ref. 3). This effort resulted in delivery to AEDC in 1969 of a nominal 5-MW segmented arc heater which after five more years of testing and development, operated at a chamber condition of 150-atm pressure and 3,500-Btu/lb enthalpy (Ref. 4).

1.3 HEAT FACILITY

In 1973, design of a nominal 40-MW d-c power supply was initiated as the first step in developing a new high-pressure, high-enthalpy ablation test facility (HEAT). Utilizing the experience gained from operating the 5-MW prototype segmented arc heater, a new

large segmented arc heater was designed, fabricated, and installed and was initially operated in June 1976. A new eight-position model injection system was also installed for model testing. The description, initial development, and calibration of this facility are presented in this report.

2.0 FACILITY DESCRIPTION

The HEAT Facility is located in the High Temperature Laboratory (HTL, Fig. 1) of the AEDC Propulsion Wind Tunnel Facility (PWT) and consists of two test cells or legs as depicted in the schematic of Fig. 2. The main test leg (H-1) will be used for ablation and combined ablation/erosion testing. The second will be used primarily for facility-oriented research and development. Both test legs share the same basic utilities including the d-c power supply capable of 40- to 60-MW output for several minutes. The air system can provide air at pressures up to 3,800 psi and flow rates up to 10 lbm/sec.

The main test leg utilizes a large segmented arc heater scaled from the AEDC prototype segmented arc heater. This prototype heater demonstrated that bulk enthalpy of the effluent stream varies from approximately 7,000 Btu/lbm at a chamber pressure of 25 atm to 3,500 Btu/lbm at 150 atm. The enthalpy profiles at the nozzle exit are essentially flat in contrast to the peak profiles characteristic of the Huels-type arc heater. A schematic of test leg H-1 is shown in Fig. 3, and a photograph of the installation is shown in Fig. 4.

The second test leg (H-2) is equipped with a nominal 12-MW Linde heater (Huels arc) for facility-oriented research and development and, if required, for ablation tests at lower enthalpies.

2.1 POWER SUPPLY

The d-c power supply consists of a three-phase, load-tap-changing transformer feeding a three-phase full-wave bridge rectifier. The rectifier consists of over 400 diodes connected in a series-parallel combination to give a maximum open-circuit voltage of 50 kv and a maximum operating current of 2,000 amp. The maximum design power of the system is 60 MW and a-c reactors, adjustable in fifteen steps up to a maximum of 23.4 ohms, are available for stabilization and load matching. Six resistor banks, each with up to 4 ohms of ballast, are used to split the arc current on up to three electrode rings at each end of the arc heater. A line diagram of the power supply is shown in Fig. 5. The power supply characteristics for 1.4 ohms and 9.0 ohms reactance without ballast resistance are presented in Fig. 6.

2.2 WATER AND AIR SYSTEMS

The arc heater components are cooled by a closed-loop demineralized water system which supplies water at pressures up to 1,500 psi and flows up to 1,300 gpm. The demineralized water is cooled by passing it through a tubed heat exchanger supplied with low-pressure raw water. The demineralized water is distributed to the arc heater electrodes and segments by nonconducting hoses connected to 4-in.-diam inlet and outlet manifolds. Filtered raw water at pressures up to 450 psi and flow rates in excess of 10,000 gpm is available for cooling other facility components.

Air is available from a large storage facility at pressures up to 3,800 psi and flow rates up to 10 lb/sec at the HEAT Facility. The airflow rates to the arc heaters vary between 0.5 to 5 lb/sec and are controlled by a remotely operated regulating system. Air is automatically injected into the arc heater upon initiation of arc current and the airflow is continuously measured by a subsonic venturi and/or a calibrated choked venturi.

2.3 LARGE SEGMENTED ARC HEATER

The large segmented arc heater was designed in Fiscal Year 1975 (FY75) and fabricated during FY76. The design was performed at AEDC and was based on the operating experience with the AEDC 5-MW segmented arc heater from FY72 through FY75 (Refs. 4 and 5)and also an analytical design study completed by Aerotherm Division of Acurex Corporation in October 1974 (Ref. 6).

The arc heater consists of a straight channel approximately 60 in. long with six transition segments and three electrode rings at each end of the channel. A photograph of the heater in operation is shown in Fig. 7, and a schematic of the configuration is presented in Fig. 8. The channel contains 204 copper segments, each electrically isolated, individually water-cooled, and capable of air injection. Each electrode ring has a magnetic spin coil surrounding the electrode liner. The coils are electrically connected in series with the arc; the polarity is selected to augment the air swirl and enhance rotation of the arc termination on the electrodes. The heater is operated with reversed polarity throughout the test series, i.e., the anode rings were the upstream electrodes. The heater and power supply are isolated from ground while the nozzle and models are electrically grounded.

Eight electrically isolated upstream segments are positioned between the anode and end cap assembly. These segments, combined with tangential air injection, prevent arc attachment to the end cap. Three isolated downstream segments provide a converging section into the nozzle throat. Two contoured nozzles have been used to date: (1) a

Mach 2.00 nozzle with a 0.625-in.-diam throat and (2) a Mach 2.65 nozzle with a 0.700-in.-diam throat. Air is introduced (1) adjacent to the electrodes, (2) in the upstream segments, and (3) distributed in the channel. Airflow rates, velocities, and injection locations were varied in order to provide proper arc operation. Swirl direction for all air stations was clockwise looking downstream.

2.4 MODEL-POSITIONING SYSTEM

Each leg of the facility is equipped with a multiple-strut, remotely controlled rotary model injection system (Figs. 9 and 10). During any given firing, from one to seven models are positioned sequentially on the test stream centerline for preset dwell times ranging from 0.5 sec to 5.0 min. The system provides a nearly constant injection velocity during the index cycle between normal stop positions and, by using 45-deg offset arms, transient calibration probes can be swept through the test stream at constant velocity. In this mode, sweep speeds from approximately 20 to 60 in./sec can be attained. Models can be alternately centered or swept through the flow in any predetermined sequence.

The model-positioning system is normally operated with the carriage in a fixed position which allows the models to rotate only laterally with respect to the nozzle exit. However, the uniform flow regions in high-pressure arc facilities are limited in size because of power limitations and the recession of an ablating model frequently moves the model nosetip out of the uniform flow region. To eliminate this problem, the entire model injection system is driven axially with a servo-controlled drive system to advance the model upstream at (essentially) the same rate at which it ablates downstream, thus holding the model front surface in the uniform flow field.

A schematic of the model advance system and a block diagram of the laser control system are presented in Fig. 10. The test unit model advance system includes a laser beam propagated through the centerline of the plasma stream and detected by a photocell sensor. When the laser beam is blocked by the model front surface, a command signal is sent to the servovalve and hydraulic cylinder to stop forward movement. When the model recedes approximately 0.002 in. and the laser beam is partially uncovered, the photocell signals the axial drive system to move forward to the null point. The model front surface is thereby kept at virtually a fixed position with respect to a predetermined test station. Feedback from the model injection system axial position sensor can be used to calculate recession rates.

This same axial drive system can be used to move (or "ramp") the model forward in the flow field and simulate reentry. This system is useful in determining the onset of transition as the model pressure is increasing. Ramp rates of about 0.5 in./sec are easily accomplished over a 5-in. length.

Control of the entire model injection system is performed using a Digital Equipment Corporation 1430 controller. This controller computer allows preprogramming of dwell times, camera sequences, and ramp rates.

2.5 ABLATION/EROSION CAPABILITY

The HEAT Facility has the capability for particle injection and acceleration for ablation/erosion testing. This unique capability is accomplished by injecting multisized particles into the gas just upstream of the nozzle and allowing the gas to drag accelerate them to high velocities. There are two systems available for particle injection (Fig. 11), each capable of providing a different range of particle concentrations. The particle/binder rod system provides positive control of dust flow rates up to 6 gm/sec. The other system provides particle concentrations by direct dust injection at dust flow rates up to 120 gm/sec. There are two nozzles presently available for particle acceleration. The smaller one is a nominal M = 1.8 nozzle with a 0.85-in. exit diameter and provides high model impact pressures at fairly high particle velocities. The second nozzle is larger, having an exit diameter of 1.4 in. This nominal M = 2.52 nozzle allows the testing of larger models at higher particle velocities but at lower impact pressures than the M = 1.8 nozzle. The calculated particle velocities for both nozzles are shown in Fig. 12.

2.6 NOZZLES

The nozzles available for the HEAT Facility are shown in Table 1. Four contoured nozzles having a 0.625-in.-diam throat and providing exit Mach numbers of 1.8, 2.0, 2.5, and 3.0 are available and also a Mach 2.65 contoured nozzle with a 0.700-in.-diam throat is available. For ablation/erosion tests, extensions are added to existing contoured nozzles to increase particle residence time to enhance the drag acceleration. This erosion capability is available with two nozzles, as shown in Table 1. It is noted that the nozzle Mach number is reduced slightly by the addition of the constant area extensions. A flared nozzle is also available for "ramping" models. This nozzle has a 0.900-in.-diam throat and a 1.80 exit Mach number. Of these available nozzles, only the 0.625-in., Mach 2.0 and the 0.700-in., Mach 2.65 nozzle flows have been calibrated.

2.7 INSTRUMENTATION

2.7.1 Facility Instrumentation

The arc heater electrical voltages and currents, cooling water flow rates and temperature rises, and air pressures and flow rates are measured to determine the arc heater performance and operating characteristics. These data are amplified and recorded

using a data acquisition system built around a Digital Equipment Corporation PDP 11/45 computer (Fig. 13). In the normal low-speed data mode approximately 100 channels, each capable of sampling at 100 points/sec, are available for facility instrumentation. Up to 65 high-speed channels, each capable of sampling at 5,000 points/sec, are available for taking data from the high-response probes. Facility data such as heater pressures, bulk enthalpy, voltage, current, and airflow rates are calculated and displayed on a CRT online and values are updated about once a second. Any of the data can be recorded on a fast direct-writing oscillograph for quick viewing of analog data. All data are recorded on magnetic tape using the facility minicomputer. Low-speed data are processed immediately after the run and printed using a 1,300-line-per-minute electrostatic printer. Data from the swept probes are reduced and plotted using the AEDC IBM 370/165 central computer.

2.7.2 Optical Instrumentation

Three high-speed cameras (100 to 10,000 frames/sec) are available for model data recovery and supplemental cameras are available as required. One of the cameras has the capability to record 10 digits of data in the film margin. Typically, the test number, run number, and the computer time are shown. In addition, up to six cameras can be selected to operate at a predetermined time on command from the model injection system controller. The photographic equipment available is presented in Table 2. Sixteen-millimeter, color motion-picture film is processed daily at AEDC, and additional copies can be made at AEDC within two days.

Television cameras monitor the models and facility during testing for rapid determination of model survivability and facility safety. These images are displayed live and recorded on video tape for later playback.

Optical pyrometers manufactured by Thermogage® are available to measure the apparent surface temperatures of models. These pyrometers have a 10- to 12-in. focal length and respond to temperatures in the 2,500°R to 7,500°R range. Up to three pyrometers can be located at different radial positions to provide maximum model coverage.

A laser velocimeter (LV) system is available to measure particle velocities in the nozzle flow. Velocities have been measured at pressure levels below 1 atm; however, the LV system is still in the development stage for measuring particle velocities in the high-pressure, high-enthalpy flows required for ablation/erosion testing.

2.7.3 Calibration Probes

A variety of probes is available to survey and calibrate the nozzle flow at various test conditions. The types of diagnostic probes available are shown in Table 3. Several of

these probes were used for the initial calibration of the HEAT Facility and the results are presented in Section 4.0.

3.0 ARC HEATER DEVELOPMENT

3.1 OBJECTIVES

The major objectives of the large segmented arc heater development were to (1) shakedown the heater and establish reliable operation at a chamber pressure of 50 atm and an arc current of 750 amp, (2) increase the operating conditions to 100 atm and 1,000 amp, and (3) operate at 150 atm and 1,500 amp. Demonstrating stable operation, component reliability, low flow contamination, and improved heater performance was the criterion for successful attainment of the objective. Operation of the heater with larger throat sizes and with multiple-powered electrode rings was another development objective.

3.2 RUN SUMMARY

The large segmented arc heater was first operated on June 18, 1976, and the data reported herein include runs performed through September 30, 1977. During this period, the heater was operated a total of 144 times. Of this total, 37 runs were of duration greater than 5 sec (the time considered necessary for a reliable energy balance) and 17 runs were longer than 15 sec (the minimum time normally required for model testing). These are summarized in Table 4 and all data reported herein are based on these 37 runs.

The heater was operated at chamber pressures ranging from 51 to 124 atm, arc currents from 670 to 1,163 amp, and enthalpies ranged from 3,330 Btu/lb at 124-atm pressure to 4,280 Btu/lb at 61 atm, all using a 0.625-in.-diam nozzle throat. Enthalpies ranged from 3,030 Btu/lb at 113 atm to 3,610 Btu/lb at 74 atm with the 0.700-in.-diam throat. A reentry simulation test was also accomplished during which the heater was initially operated at 61 atm for 6 sec and then the heater pressure was increased to 124 atm in 8 sec, then calibration models were swept through the flow twice. A time history of the chamber pressure for this run is presented in Fig. 14.

Over 100 short runs generally ranging in length from 2 to 5 sec were made during development of the heater. These runs were used to check out heater operation resulting from changes in hardware configurations or test conditions. The heater operation was completely stabilized within 3 sec at all conditions; however, at least 5 sec were required for the cooling-water temperature transient to disappear. Once successful operation was verified during the checkout runs, longer energy balance runs (>5 sec) were then generally successful. Most of the hardware development was conducted using these short

checkout runs, then longer runs were used to verify the results of the short runs and to obtain performance data. All major heater development was accomplished with a 0.625-in.-diam throat, although several runs were made with a 0.700 throat.

The first user test was conducted in July and August 1977 to calibrate the facility flow with instrumented probes. The test was successful and typical calibration results are presented in Section 4.0. The heater was operated at four test conditions for this calibration test:

Test Condition	d*, in.	p_o, atm	I, amp	H_{oB}, Btu/lb
1	0.625	75	950	4,000
2	0.625	115	950	3,500
3	0.700	74	990	3,500
4	0.700	113	1,000	3,000

3.3 PROBLEM AREAS

Several problems have been encountered during operation and development of the heater. Most of these problems have been solved or at least partial solutions found.

3.3.1 Improper Arc Attachment to Electrodes

The tendency for the arc to attach to the upstream or downstream edge of a ring electrode is quite common in a segmented arc heater. When this occurs, wall arcing and overheating of adjacent components result. Increased air injection at the affected location has been reasonably effective in controlling erosion in these areas. Also, on some high-voltage runs, the arc attached to the upstream end cap rather than to the anode ring and then tracked along the wall of the upstream segments back to the anode ring (see Fig. 8). Air injection immediately downstream of the end cap was successful in eliminating this problem.

3.3.2 Dual Electrode Operation

The arc current was divided between two electrode rings on several runs to allow higher current operation and reduce electrode erosion. Division of current was accomplished at both the anode and cathode rings, and in each case only two adjacent rings were powered. The current at each electrode was controlled by the amount of external resistance in series with that electrode.

Dual anode operation resulted in a majority of the arc attaching to the downstream anode ring and then a portion of this current transferring to the adjacent upstream

powered electrode by arcing across the air gaps between them. Increased air injection between these electrodes decreased the electrode erosion caused by the improper arc attachment. However, the large amount of air required to reduce the erosion to an acceptable level extinguished the arc on the upstream anode ring. This resulted in overheating and failure of tapered segments immediately downstream of the anodes. Dual-powered anode operation was discontinued because of other priority work.

Dual cathode operation has been accomplished successfully on many runs. The arcing between electrodes was less severe at the cathodes, and additional air injection has been successful in keeping the erosion to an acceptable level. However, the additional air required in the cathode area has reduced the heater performance slightly.

3.3.3 Wall Arcing on Upstream Tapered Segments

Tapered segments were destroyed when the tangential velocity of the air at the wall in the anode area dropped below an acceptable level. A substantial air circulation velocity is required to provide a protective cold air layer between the arc and the tapered wall which prevents segment wall arcing and overheating. A computer program (to be published) was developed by Dr. Gordon Cann, a consultant to ARO, Inc., to calculate the circulation level in the heater based on the air injection configuration. Swirl rings were then changed in the anode area to increase the tangential velocity of the air at the upstream end of the heater, and no further problem with arcing between the upstream tapered segments has been encountered.

3.3.4 Wall Arcing in Straight Segment Modules

On several runs, segment-to-segment arcing in the straight modules caused considerable segment erosion or burnout; as a result, flow contamination was visible at the nozzle exit. The exact conditions which lead to the arcing are unknown, but the evidence indicates the heater is more susceptible to this problem as the power input and throat size are increased. However, the wall arcing has been essentially eliminated at pressures below 115 atm with a 0.625-in.-diam throat by distributing air in small quantities along the entire straight section of the heater. The distributed air provides a film of cold air between the arc and the wall.

3.3.5 External Arcing

External arcing occurred in the anode area on several runs. A capacitor network was installed across the anode spin coils to reduce voltage spikes caused by the interaction of the coil magnetic field with high-frequency current fluctuations in the heater. The external arcing was then greatly reduced, but not completely eliminated. A 500-Ω resistor was connected between each segment pair with the purpose of minimizing the nonlinear

axial voltage distribution caused by the electrical coupling of the segments to ground through the cooling water. The arc heater starting characteristics are unaltered, and since addition of the resistors no external arcing on the heater has been observed.

3.4 HEATER PERFORMANCE

The arc heater performance for all runs of length greater than 5 sec is summarized in this section. Data with a 0.625-in.-diam throat and a 0.700-in.-diam throat are presented separately. The heater data are compared with a modified correlation program formulated by Aerotherm Division, Acurex Corporation (Refs. 4 and 6) and the sonic flow enthalpy equation (Ref. 7). These relationships are listed below:

$$V_{corr} = 430\left(\frac{L}{D}\right)^{0.75} \dot{m}^{0.4} p_o^{0.165}, \text{ volts} \tag{1}$$

$$H_{corr} = 4.818\left(\frac{I}{\dot{m}}\right)^{0.5}\left(\frac{L}{D}\right)^{0.825} p_o^{0.1}, \text{ Btu/lb} \tag{2}$$

$$\frac{\dot{m}}{A^* p_o} = 280\, H_s^{-0.397} \tag{3}$$

where

L = Arc channel length, in.

D = Channel bore diam, in.

$\dot{m}$ = Air mass flow rate, lb/sec

p_o = Total pressure, atm

I = Arc current, amp

A^* = Sonic throat area, ft^2

H_s = Sonic flow enthalpy, Btu/lb

H_{corr} = Calculated enthalpy (Eq. 2), Btu/lb

V_{corr} = Calculated arc voltage (Eq. 1), V

The correlation was based on data obtained from the 5-MW segmented arc heater which is presented in Ref. 4.

3.4.1 Performance with 0.625-in.-diam Throat

Figure 15 presents the enthalpy data obtained at various chamber pressures. Also shown are the calculated enthalpies based on the correlation Eqs. (2) and (3) for arc currents of 600, 1,000, and 1,500 amp. The measured enthalpies are higher than the correlation values at all pressures and arc currents tested.

Heater voltage and chamber pressure data are shown in Fig. 16, and the enthalpy and efficiency data are shown in Fig. 17 as a function of the heater air mass flow rates. For all parameters, the measured levels are higher than the calculated values as shown below:

Parameter Compared	Ratio, Measured to Calculated, Average
Voltage	1.04
Total Pressure	1.13
Enthalpy	1.30
Efficiency	1.22

3.4.2 Performance with a 0.700-in.-diam Throat

The measured enthalpy as a function of heater pressure is presented in Fig. 18 for a 0.700-in.-diam nozzle throat, and correlation values based on the small segmented heater data are shown for comparison. While the measured enthalpies are higher than the calculated enthalpies, the data do lie along lines of constant current.

Heater voltage, pressure, enthalpy, and efficiency are presented in Figs. 19 and 20. The voltage is very close to the predicted level; however, measured pressure, enthalpy, and efficiency were significantly higher than calculated. This deviation is shown below:

Parameter Compared	Ratio, Measured to Calculated, Average
Voltage	0.98
Total Pressure	1.13
Enthalpy	1.32
Efficiency	1.33

3.4.3 Sonic Flow Enthalpy

In order to determine if the sonic flow equation developed by Winovich (Ref. 7) was applicable to the large segmented arc heater, a logarithmic plot of m/A^*p_o versus enthalpy is presented in Fig. 21 for both the 0.625- and 0.700-in.-diam throat data. A least squares fit of the data resulted in the following expression:

$$\frac{\dot{m}}{A^* p_o} = 271\, H_s^{-0.395} \tag{4}$$

This curve fit and the Winovich equation are both shown along with the heater data in Fig. 21. Either Eq. (3) or (4) can be used to calculate a reasonably accurate enthalpy for this heater.

4.0 FACILITY CALIBRATION

The facility was thoroughly calibrated at a nominal 75-atm and 115-atm heater stagnation pressure. Two nozzles were used for the calibration, a Mach 2.0 (d^* = 0.625 in.) and a Mach 2.65 (d^* = 0.700 in.). The M = 2.0 (d_e = 0.85 in.) nozzle will be used primarily for ablation testing and the M = 2.65 (d_e = 1.40 in.) nozzle will be used for ablation/erosion testing and transpiration-cooled nosetip testing. Pressure and heat-transfer measurements were made at the following axial stations: 0.05, 0.25, 0.50, and 1.00 in. from the nozzle exit. This calibration program was sponsored by the Air Force Materials Laboratory and the Technical Evaluator was AVCO, Inc. The data presented here are only part of this calibration program and will not be analyzed in great detail. The reader is referred to the AFML contractor report to be published in the near future.

4.1 M = 2.0 CALIBRATION

Pressure and heat-transfer probes were used to calibrate the nozzle flow. An additional run was made at 124-atm heater pressure to complete the data envelopes. A "standard" 0.25-in.-radius, 10-deg cone calorimeter and a 0.15-in.-radius, 10-deg cone calorimeter were swept through the flow twice on each run to determine spatial nonuniformities in the flow. Several facility runs were made and data collected at these test conditions.

4.1.1 Pressure

Figure 22 represents the impact pressure data taken at arc heater pressures of 75 and 115 atm. Note that the pressure profiles are flat in the test rhombus (upstream of the expansion wave from the nozzle lip) and represent a significant flow size at high

pressures. A plot of the centerline pressure axial distribution (Fig. 23) shows a near constant pressure field that decreases downstream of the expansion fan. Also shown are data at an arc heater pressure of 124.6 atm. The measured radial pressure profiles at 124.6 atm are similar to those presented in Fig. 22 for the lower pressures.

4.1.2 Heat Transfer

The radial heat-transfer distributions were relatively flat within the test rhombus as seen in Figs. 24 and 25. There appears to be timewise fluctuations in heat transfer at both operating pressures, independent of the size calorimeter used. There is no heat-transfer peaking or spiking characteristic of the more conventional high-voltage arc heaters used by all other high-pressure ablation test facilities in this country.

The nominal centerline hot wall heat-transfer data are plotted versus axial distance from the nozzle exit in Fig. 26 for the two calorimeters utilized. Heat-transfer rates approaching 20,000 Btu/ft^2-sec were measured at the exit of the nozzle with the R_N = 0.25-in. calorimeter. Rates as high as 27,000 Btu/ft^2-sec were measured with the R_N = 0.15-in. calorimeter. The increase in the heat transfer with increasing distance from the nozzle exit is probably caused by the increase in the free-stream turbulence downstream of the nozzle exit. The decrease in heat transfer beyond the flow rhombus is caused by the effect of the decreasing pressure (Fig. 23) on the heat transfer.

4.2 M = 2.65 CALIBRATION

This nozzle was also calibrated using the pressure probe and one R_N = 0.25-in. calorimeter. A second calorimeter (R_N = 0.50 in.) was used to obtain additional data at two axial stations. Each probe was swept through the flow twice on each run to verify the profiles.

4.2.1 Pressure

The radial pressure profiles of Fig. 27 clearly show that the flow field in the test rhombus is relatively uniform up to approximately the 1.00-in. axial station. The axial pressure distribution shows a slightly increasing stagnation pressure downstream of the nozzle exit (Fig. 28). The nozzle was designed for the 115-atm arc heater condition, but the nozzle boundary layer appears to be thicker than expected resulting in an increase in flow stagnation pressure.

4.2.2 Heat Transfer

The R_N = 0.25-in. and R_N = 0.50-in. calorimeters were used to measure radial and axial heat-transfer profiles of the nozzle jet. The R_N = 0.50-in. calorimeter was used at

only two axial stations (X = 0.05 and 0.50 .)The radial profiles shown in Fig. 29 look very similar to the M = 2.0 nozzle heat-transfer profiles and show no sign of peaking on the centerline. There appears to be some timewise fluctuations in the flow, especially at the higher pressure. The axial heat-transfer distributions are shown in Fig. 30 for both calorimeters and, generally, the measured heat-transfer rates increased slightly with increasing distance from the nozzle exit within the test rhombus. There is very little difference between heat-transfer rates measured with the small and large nose radius calorimeters. This is thought to be the result of free-stream turbulence influencing the measured heat transfer.

4.3 ENTHALPY

AEDC utilizes three methods to determine the so-called free-stream stagnation enthalpy. The most common method is to make an overall energy balance by measuring the arc heater input power, air mass flow rate, and the cooling-water losses to determine the "bulk enthalpy." This bulk, or the average, enthalpy does not accurately indicate the enthalpy distribution or, in particular, the centerline value. The second enthalpy-measuring technique utilizes the AEDC transient enthalpy probe to measure the radial distribution. This probe, described in Ref. 8, has been used for a number of years and provides a direct measurement of flow stagnation enthalpy called the "measured enthalpy." Finally, an enthalpy can be calculated from the measurement of heat-transfer rates and flow stagnation pressure. Normally, the standard Fay and Riddell laminar flow equation relating enthalpy to the heat transfer is used with no corrections for free-stream turbulence. It is generally accepted that all arc heaters generate some level of free-stream turbulence resulting in a higher measured heat-transfer rate than calculated. The calculated enthalpy is called "inferred enthalpy" and should be used to determine the heat-transfer rates to test specimens in the flow. If one needs to know the chemistry of the flow behind the bow shock, the "measured enthalpy" should be used.

Figures 31 and 32 show the enthalpy obtained from the three methods for the M = 2.0 and M = 2.65 nozzles. It is concluded that the "inferred enthalpy" is 75 percent higher than the "measured enthalpy" at the high-pressure condition for the M = 2.0 nozzle because of the presence of free-stream turbulence. The measurements at the exit of the larger M = 2.65 nozzle show a 100-percent increase in "inferred enthalpy" when compared to the "measured enthalpy." These data are presented in this manner to point out to a prospective facility user that extreme care must be taken when using the enthalpy from one facility to compare with the enthalpy from another facility. The "measured enthalpy" using the transient enthalpy probe is unique to the AEDC HEAT Facility and is considered an extremely important measurement which should be included in all facility calibrations.

5.0 CONCLUDING REMARKS

The HEAT Facility was developed to provide ablation and ablation/erosion simulation of reentry flight conditions. The facility is operational and all major components have been brought online. The power supply has been operated in excess of 20 MW stably with an arc heater load and has been stress checked to 50 kv and 2,000 amp. The model-positioning system has been programmed for a variety of injection sequences, and both calibration and ablation models have been swept through or positioned in the flow.

A large segmented arc heater has been fabricated, installed, and operated at chamber pressures up to 124 atm. The measured enthalpies ranged from 3,330 Btu/lb at 124-atm heater pressure to 4,280 Btu/lb at 61 atm when the heater was operated with a 0.625-in.-diam nozzle throat. The heater has been also operated at chamber pressures up to 115 atm with a 0.700-in.-diam nozzle throat, and the arc current was divided successfully between two cathode rings. The heater has been operated 144 times, of which 37 runs were longer than 5 sec. Models were injected on most of the longer runs.

The first user test has been successfully completed and consisted of calibrating the flow with swept probes at four test conditions. The pressure and heat-transfer profiles were relatively flat which is characteristic of a segmented arc heater. The nozzle flow was extremely clean and free of contamination.

REFERENCES

1. Brown, S. G. A. and Patton, J. B. "Calibration and Operation of the Linde Model N4000 Arc Heater with 1/2- and 3/8-Inch Diameter Constrictors." AEDC-TR-65-102 (AD465346), June 1965.

2. Horn, D. D. "Ablation Testing for Tasks 3, 4, and 5 of the Re-entry Systems Environmental Protection (RESEP) Program in the AEDC 5-MW Arc Heater Test Unit." AEDC-TR-68-154 (AD837841), August 1968.

3. Richter, R. "Ultrahigh Pressure Arc Heater Studies." AEDC-TR-69-180 (AD859053), September 1969.

4. Horn, D. D. and Smith, R. T. "Results of Testing the AEDC 5-MW Segmented Arc Heater at Pressures up to 171 atm." AEDC-TR-75-127 (ADA017288), November 1975.

5. Horn, D. D. and Brown, S. G. A. "Results of Testing the AEDC 5-MW Segmented Arc Heater." AEDC-TR-74-108 (ADA002313), December 1974.

6. Nicolet, W. E., Shepard, E. C., et al. "Analytical and Design Study for a High-Pressure, High-Enthalpy Constricted Arc Heater." AEDC-TR-75-47 (ADA012551), July 1975.

7. Winovich, W. "On the Equilibrium Sonic-Flow Method for Evaluating Electric-Arc Air-Heater Performance." NASA TN D-2132, March 1964.

8. Smith, R. T., MacDermott, W. N., and Giltinan, T. L. "A Transient Enthalpy Probe for the Calibration of High Heat Flux Ablation Facilities." AEDC-TR-74-116 (ADA003950), January 1975.

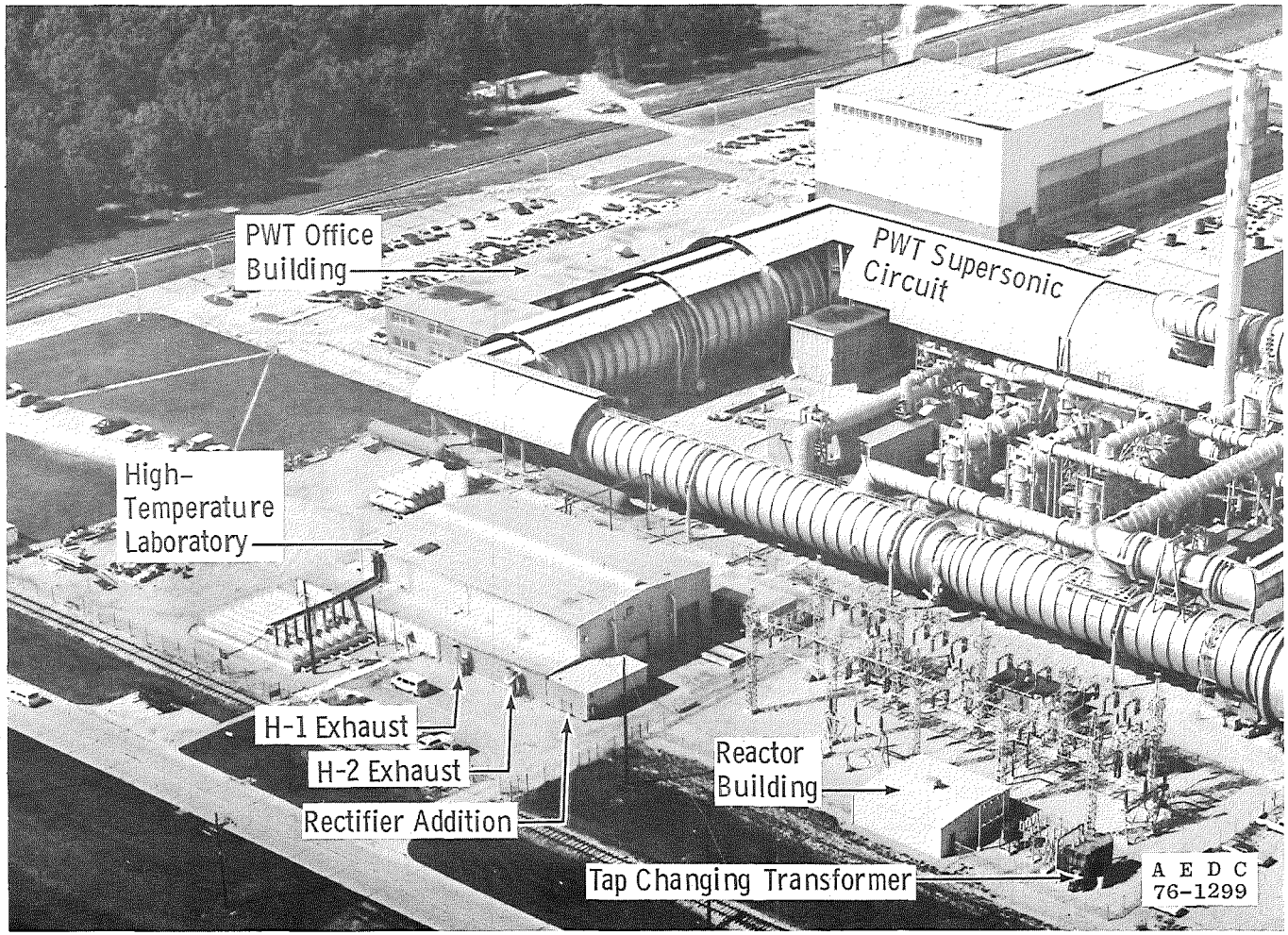

Figure 1. Aerial photograph of the AEDC High-Temperature Laboratory.

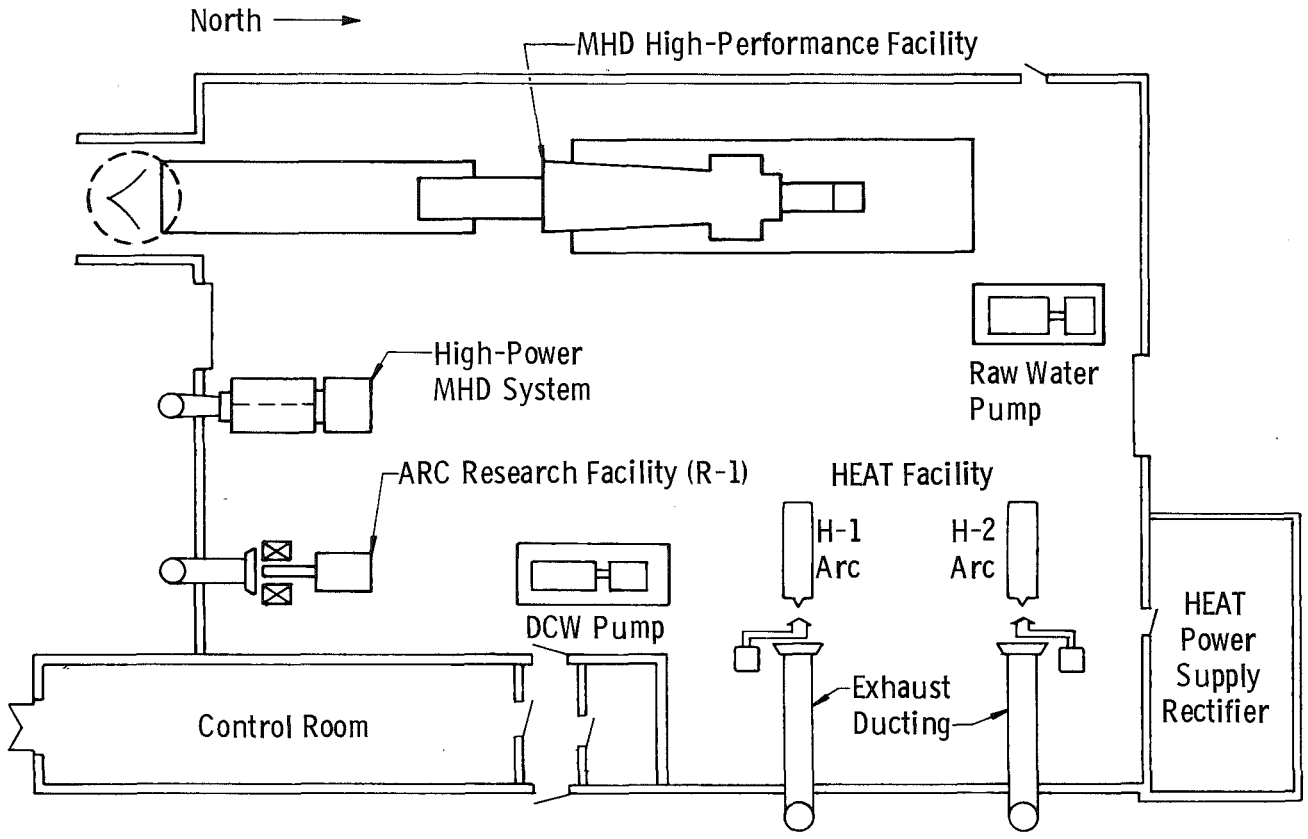

Figure 2. Layout of the AEDC High-Temperature Laboratory showing the location of the HEAT Facility.

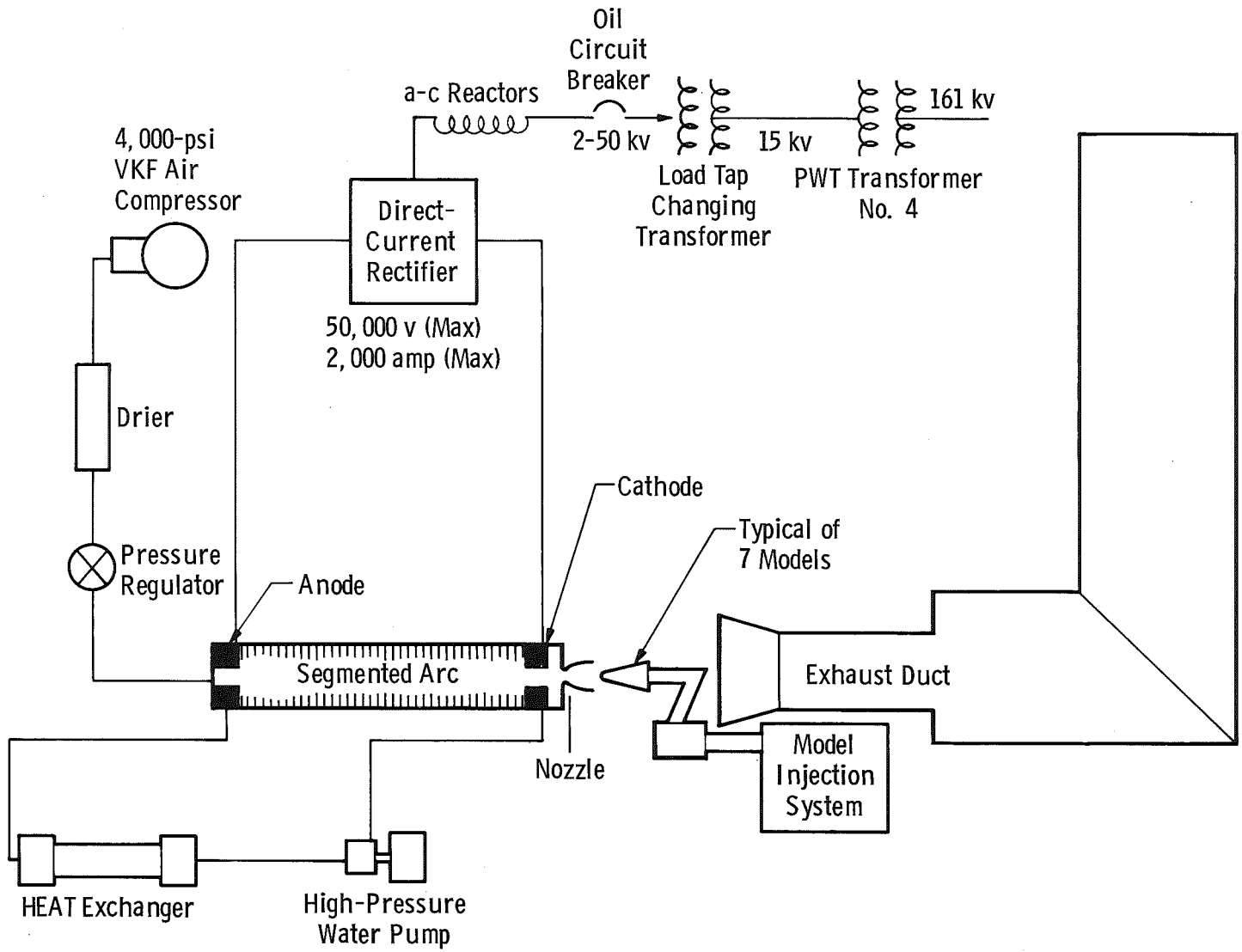

Figure 3. Schematic of the HEAT Facility test leg H-1.

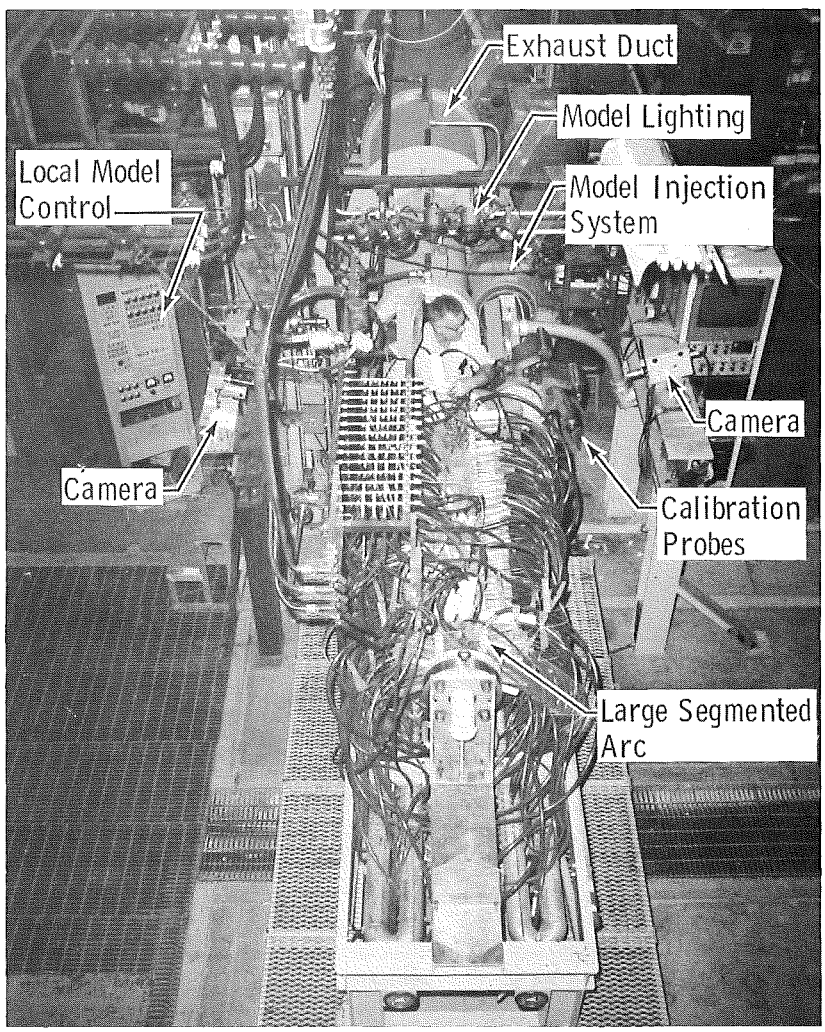

Figure 4. Photograph of H-1 test leg.

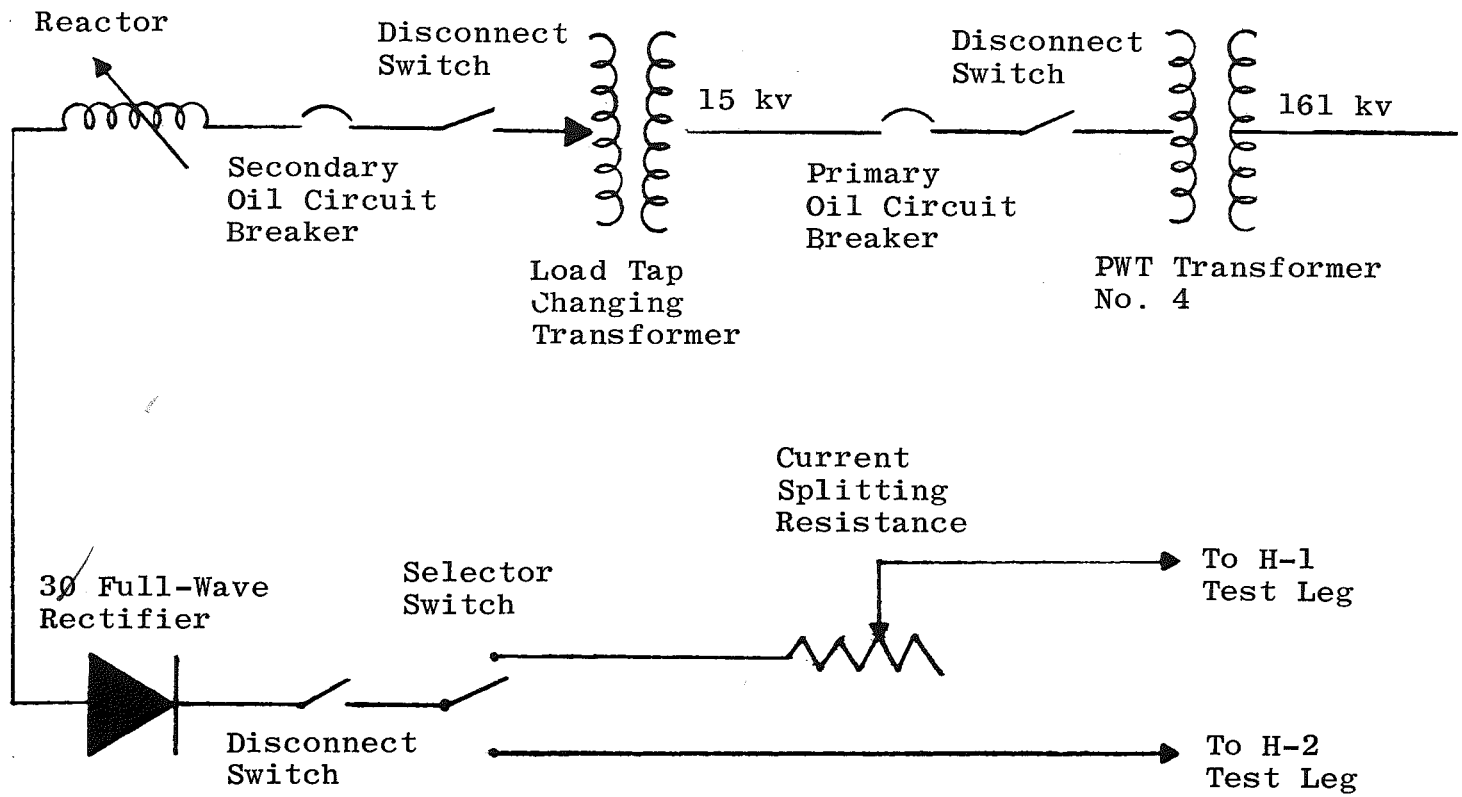

Figure 5. One-line diagram of HEAT Facility power supply.

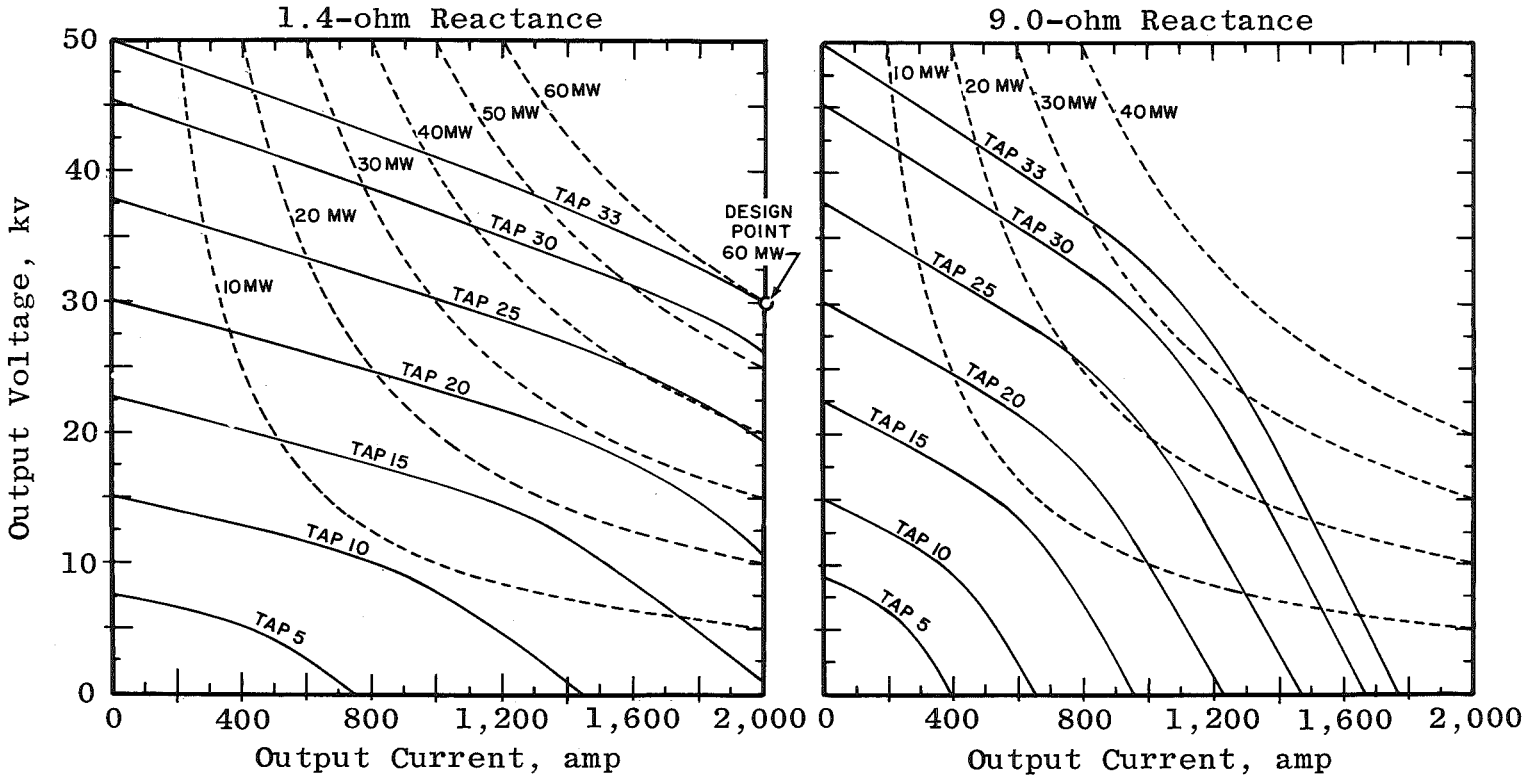

Figure 6. HEAT power supply characteristics.

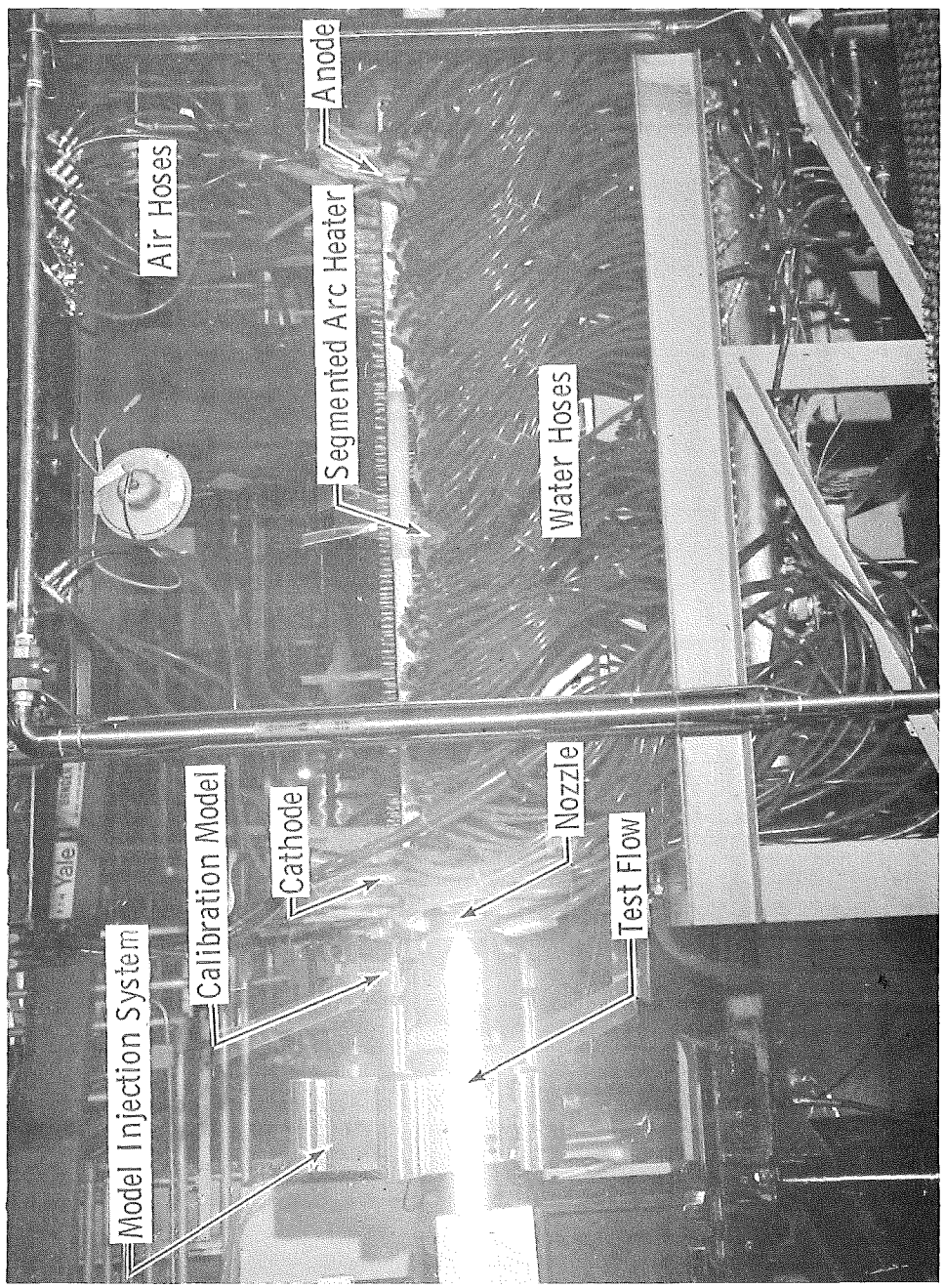

Figure 7. Photograph of HEAT (H-1) Facility.

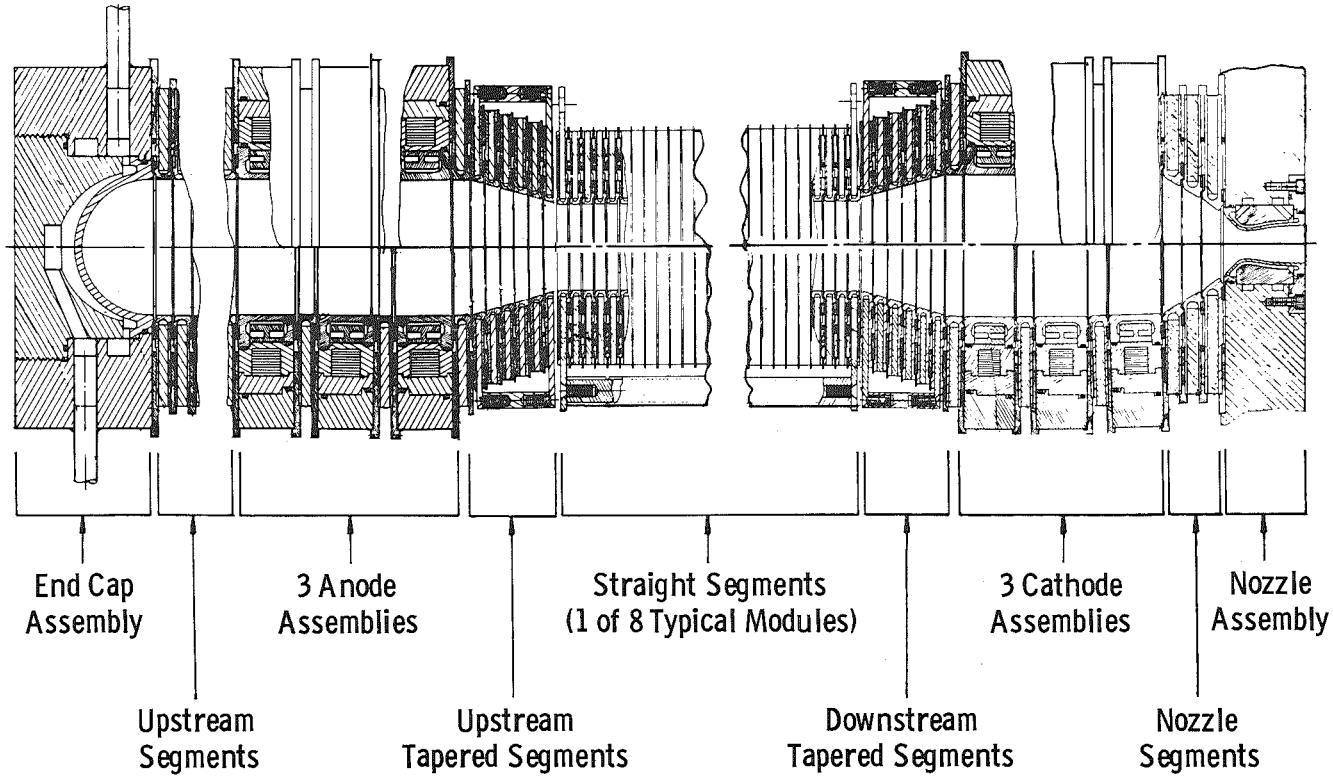

Figure 8. Sketch of the HEAT segmented arc heater.

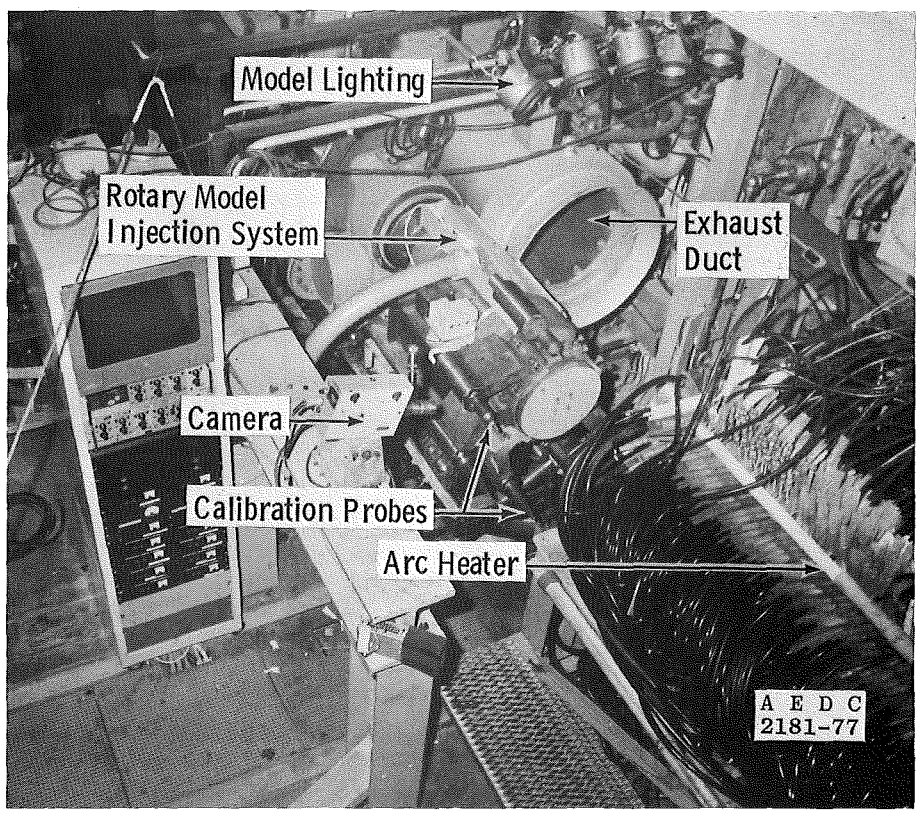

Figure 9. Rotary model injection system for H-1.

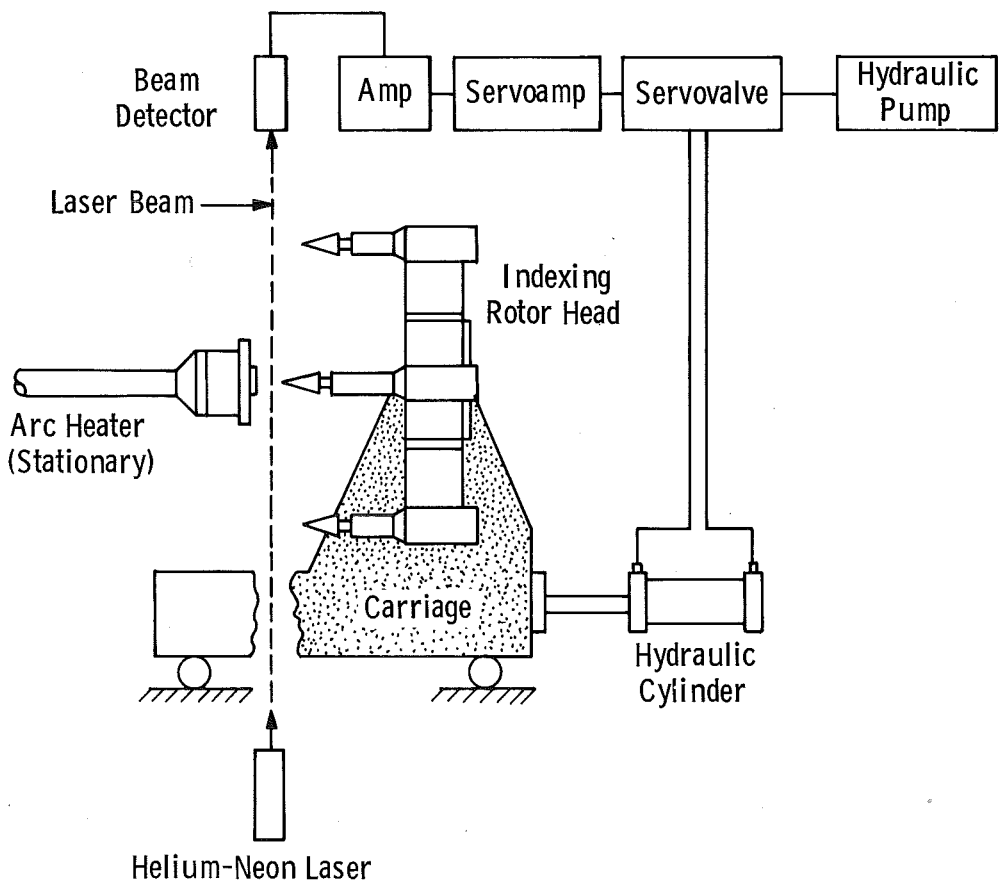

Figure 10. Laser-controlled model advance system.

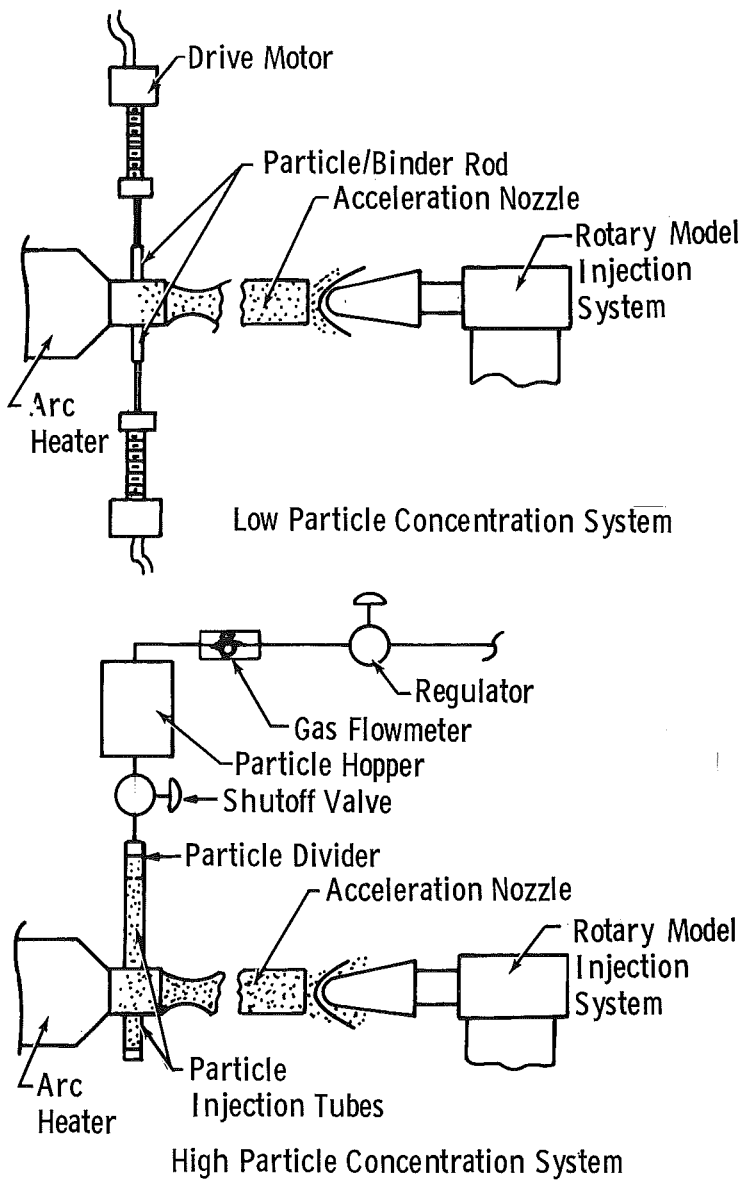

Figure 11. Available particle injection systems.

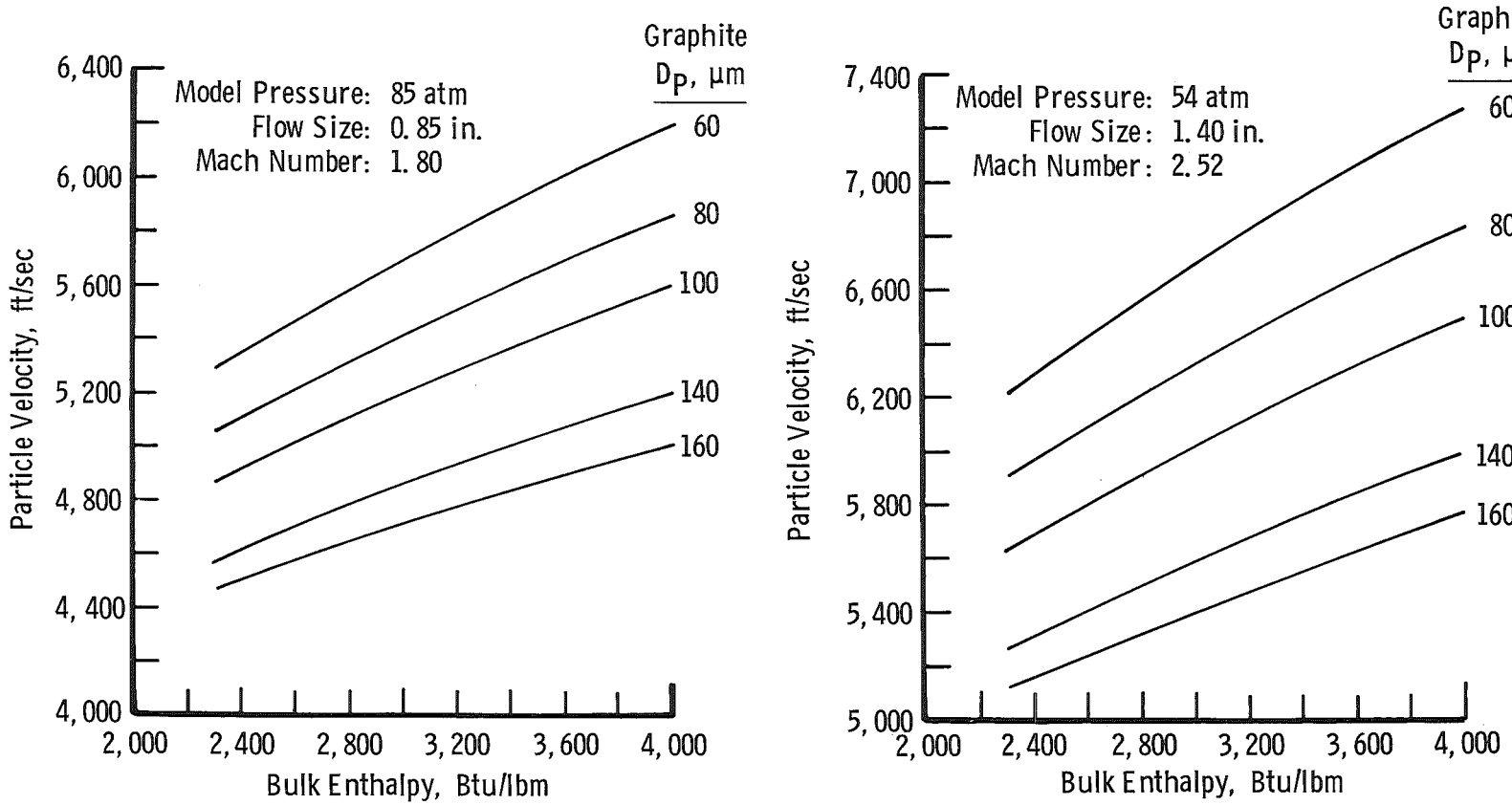

Figure 12. Particle velocity for various bulk enthalpies and particle sizes for arc heater pressure of 120 atm.

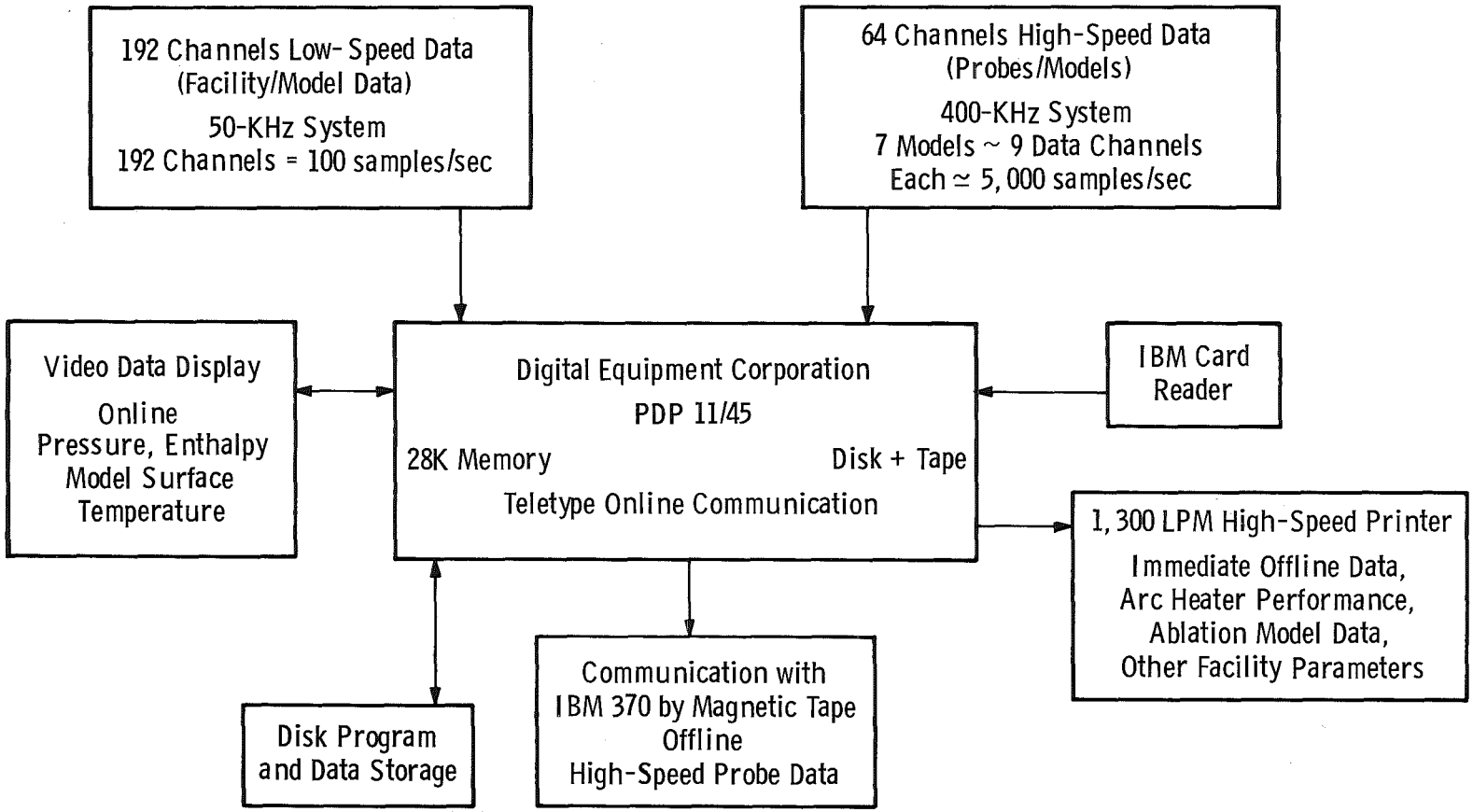

Figure 13. HEAT Facility data acquisition system.

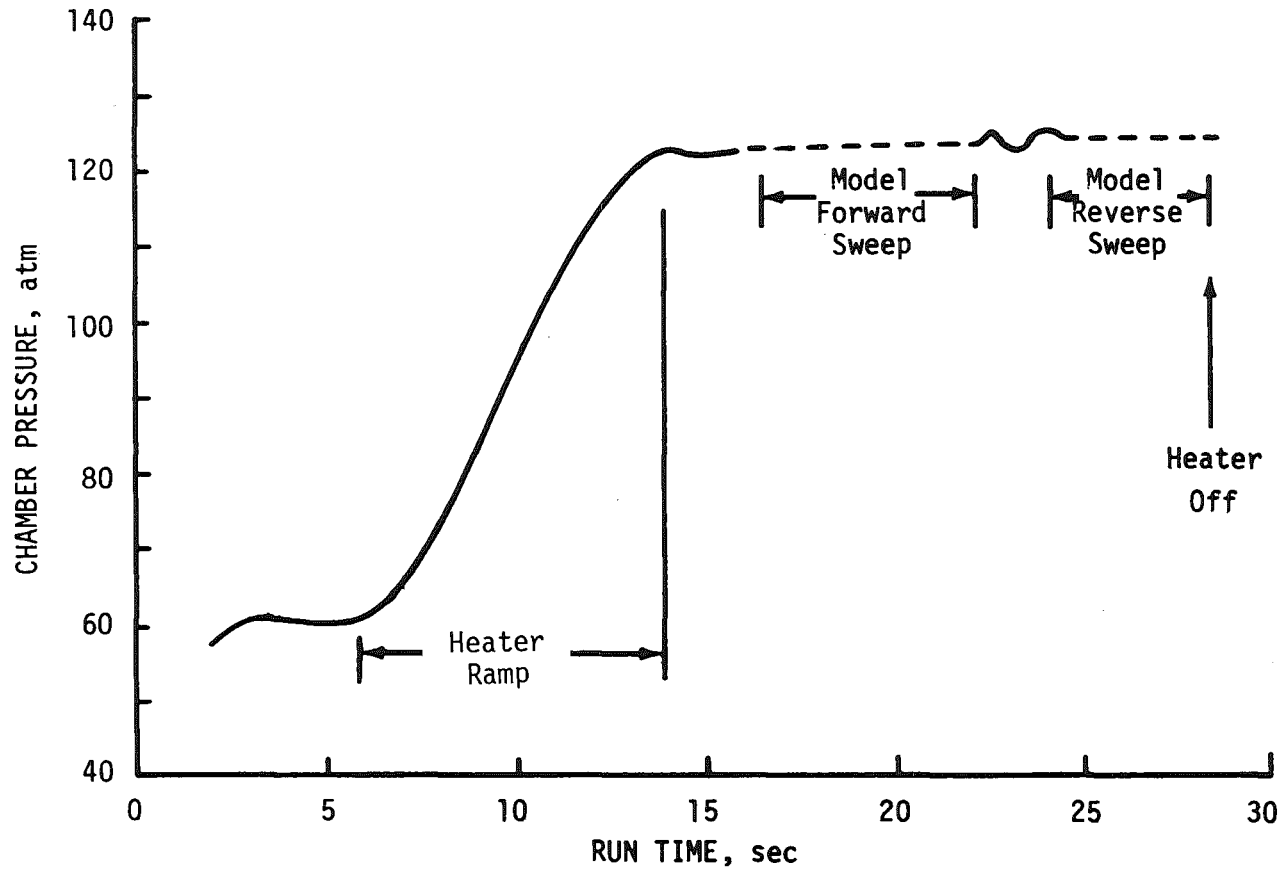

Figure 14. HEAT operation in "ramp" mode.

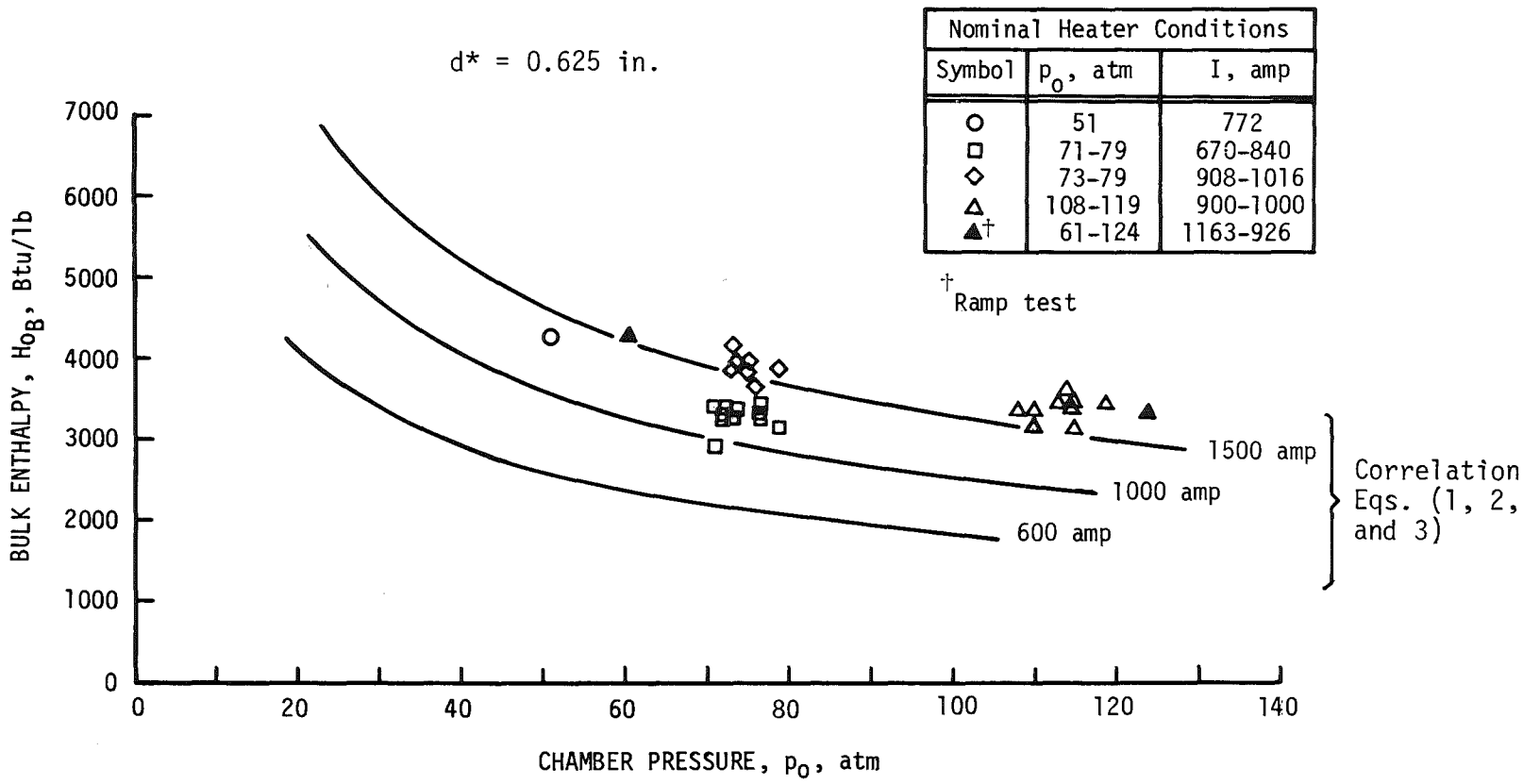

Figure 15. Large segmented arc heater enthalpy for d* = 0.625 in.

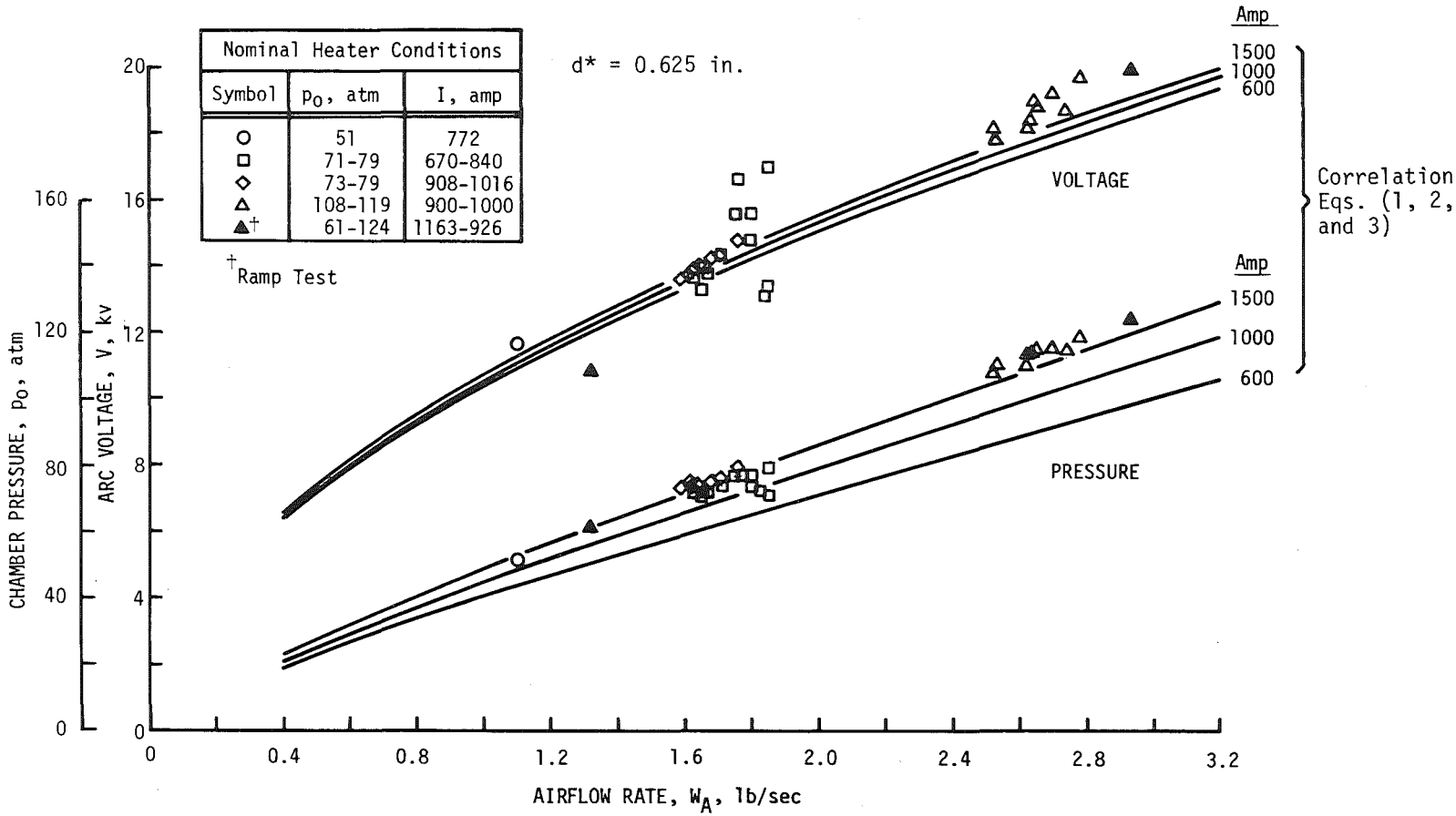

Figure 16. Heater pressure and voltage for d* = 0.625 in.

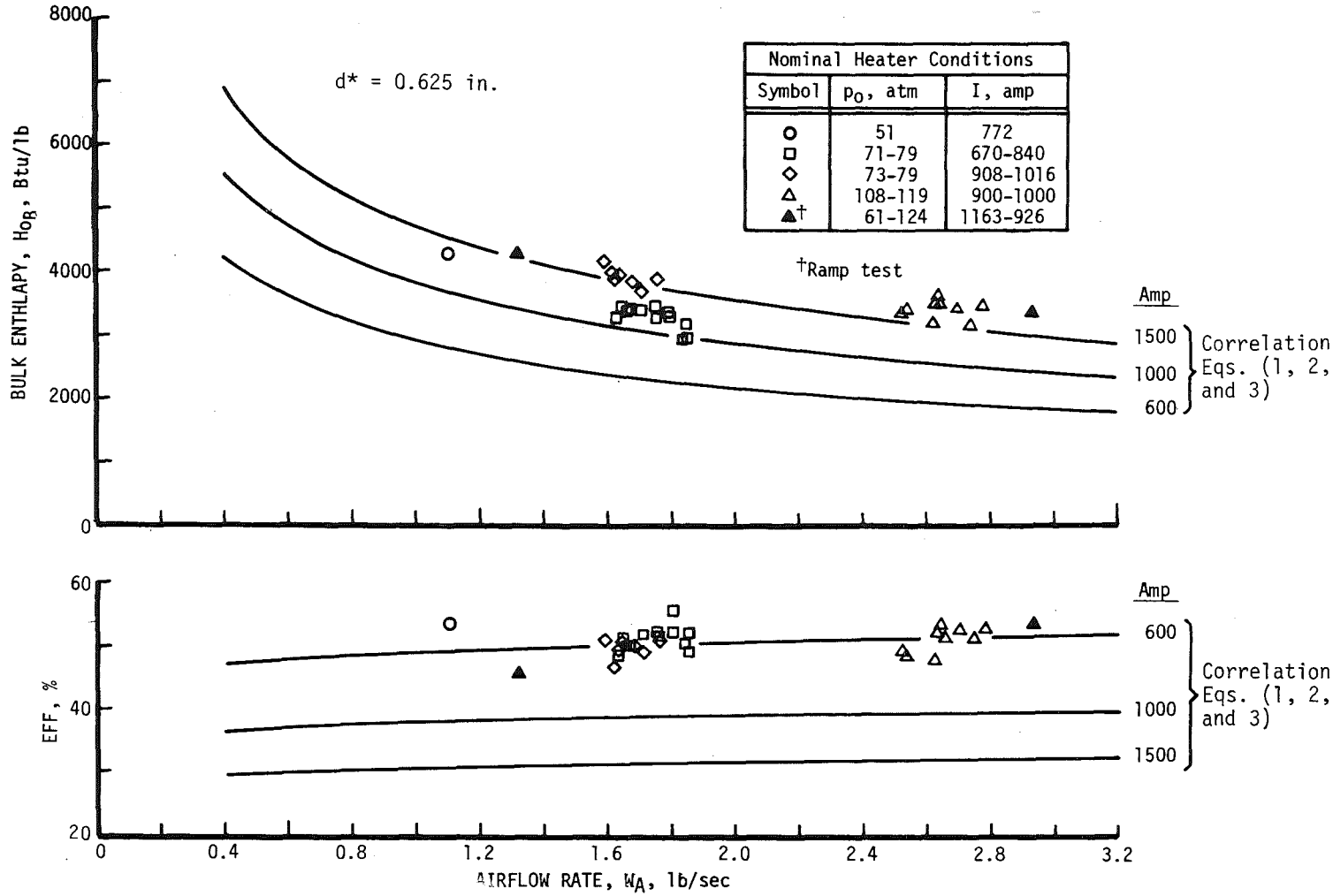

Figure 17. Heater enthalpy and efficiency for d* = 0.625 in.

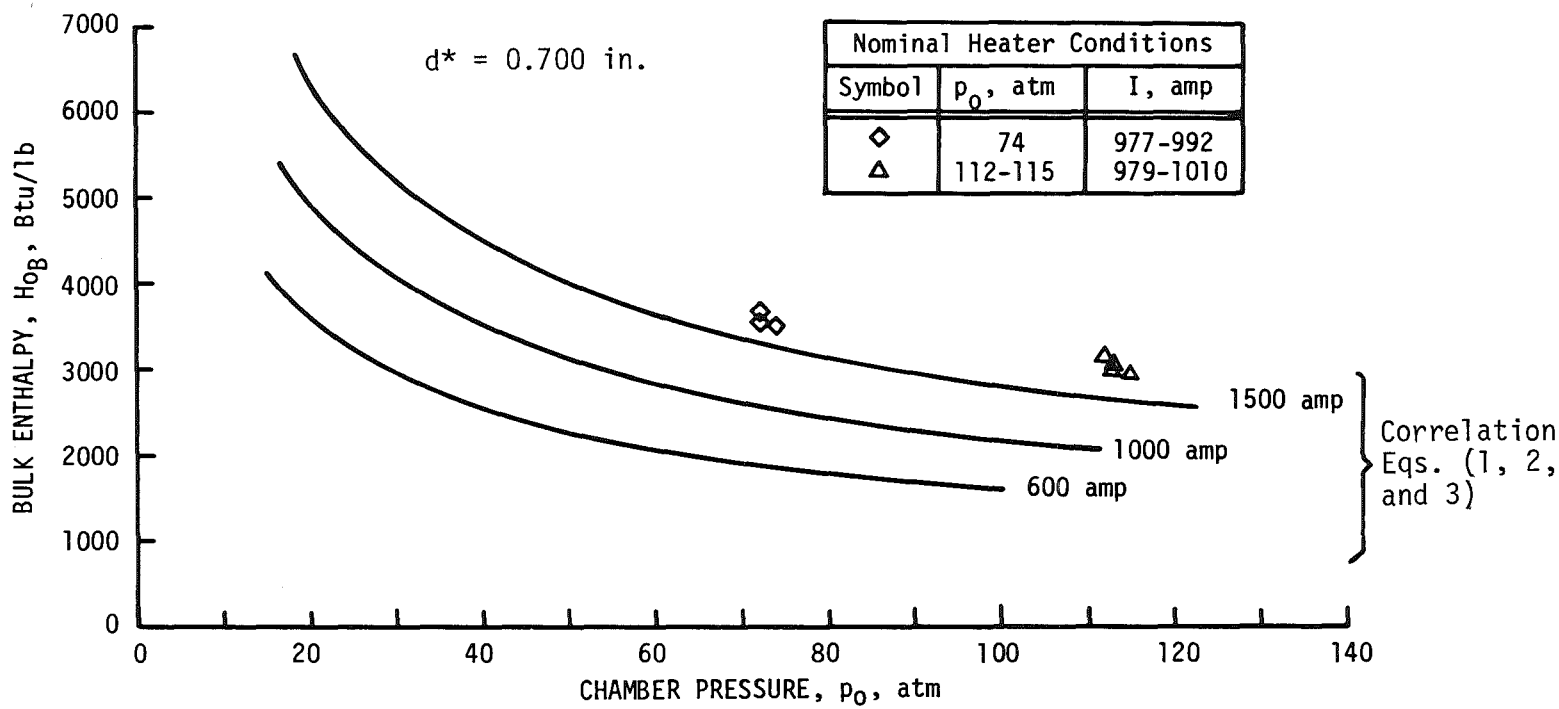

Figure 18. Heater enthalpy for various chamber pressures, d* = 0.700 in.

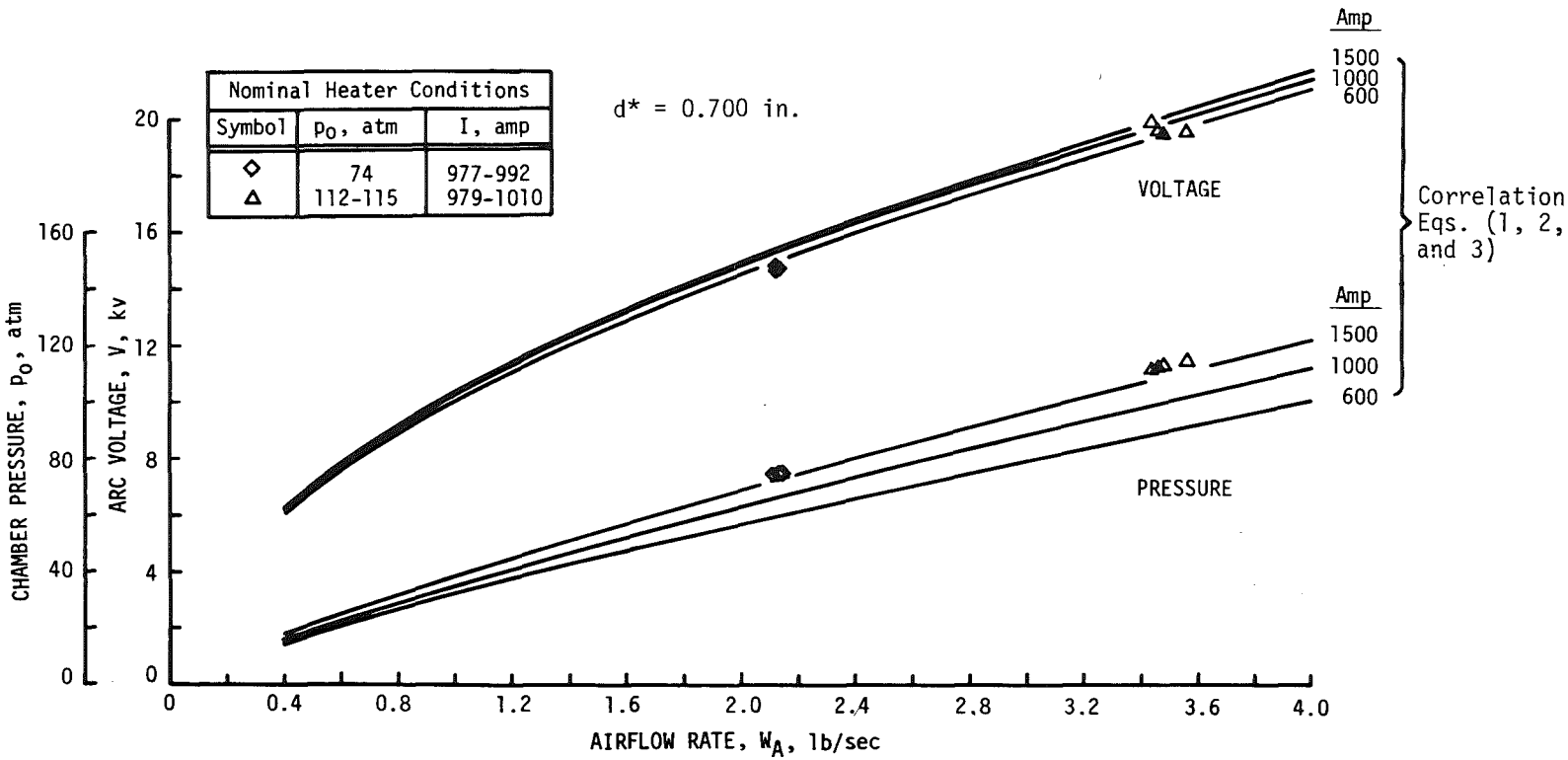

Figure 19. Heater pressure and voltage for d* = 0.700 in.

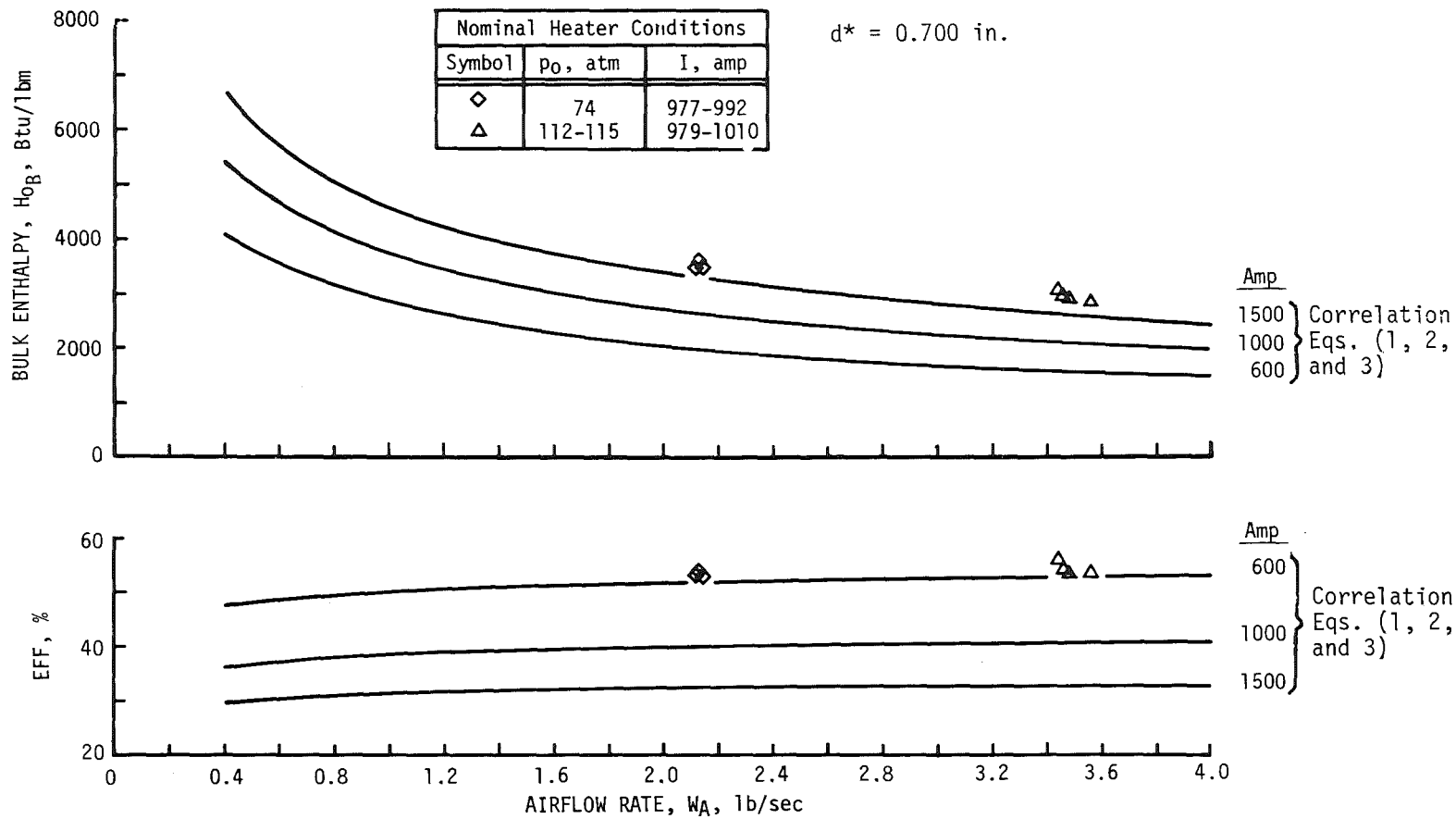

Figure 20. Heater enthalpy and efficiency for d* = 0.700 in.

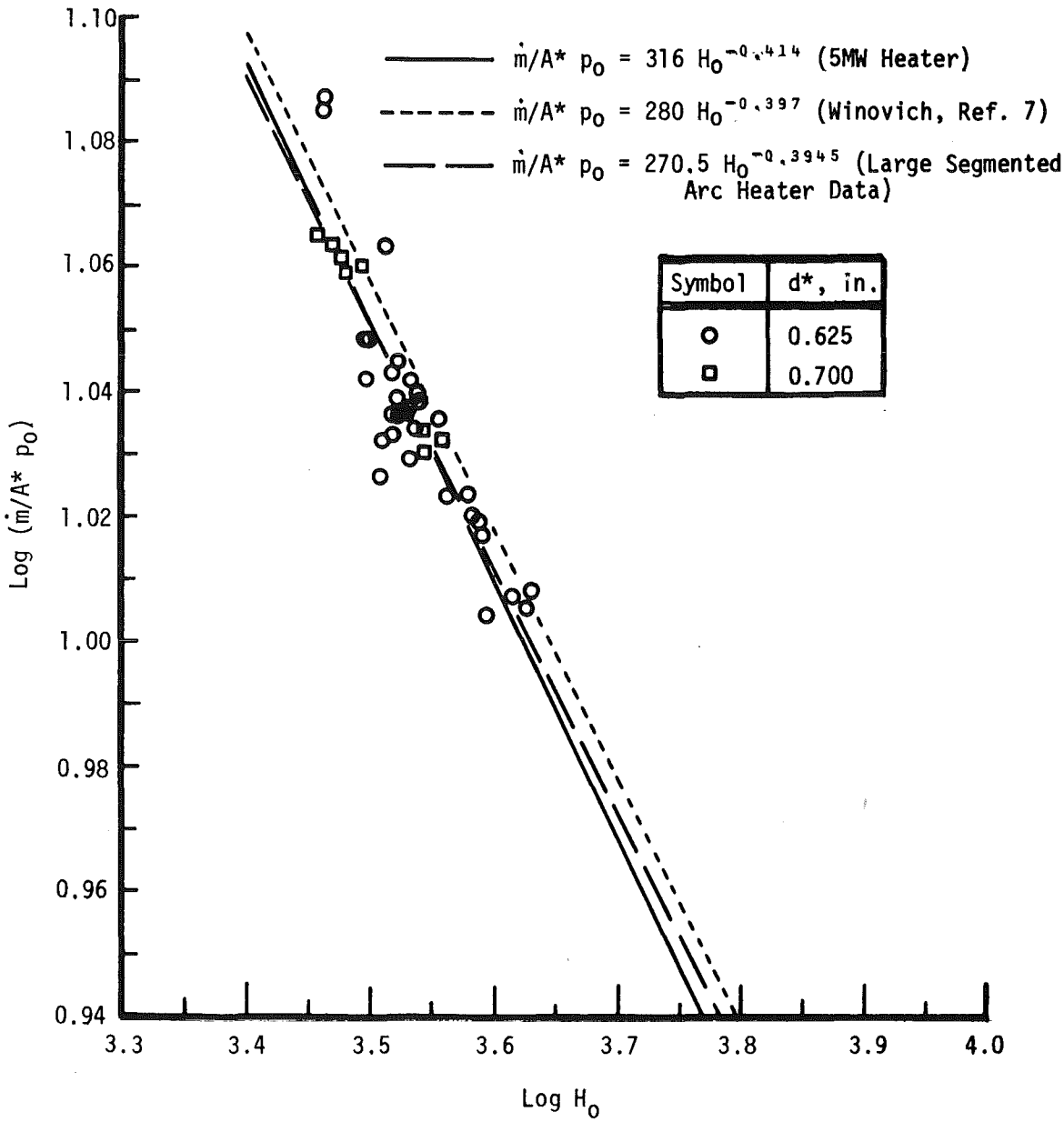

Figure 21. Comparison of arc heater data with sonic flow equation.

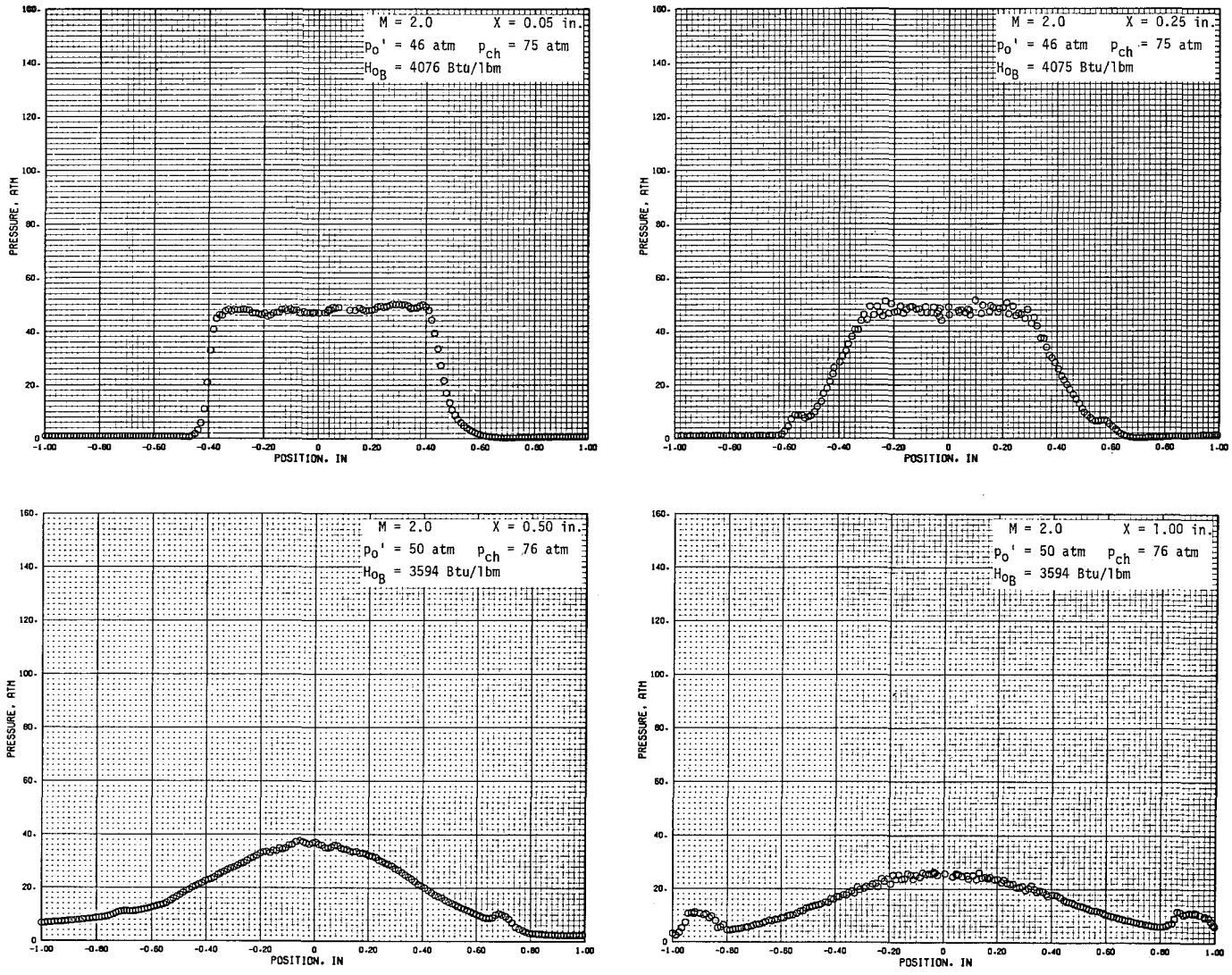

Figure 22. Radial pressure profiles, M = 2.00, d* = 0.625 in., d_e = 0.850 in., and I = 950 amp.

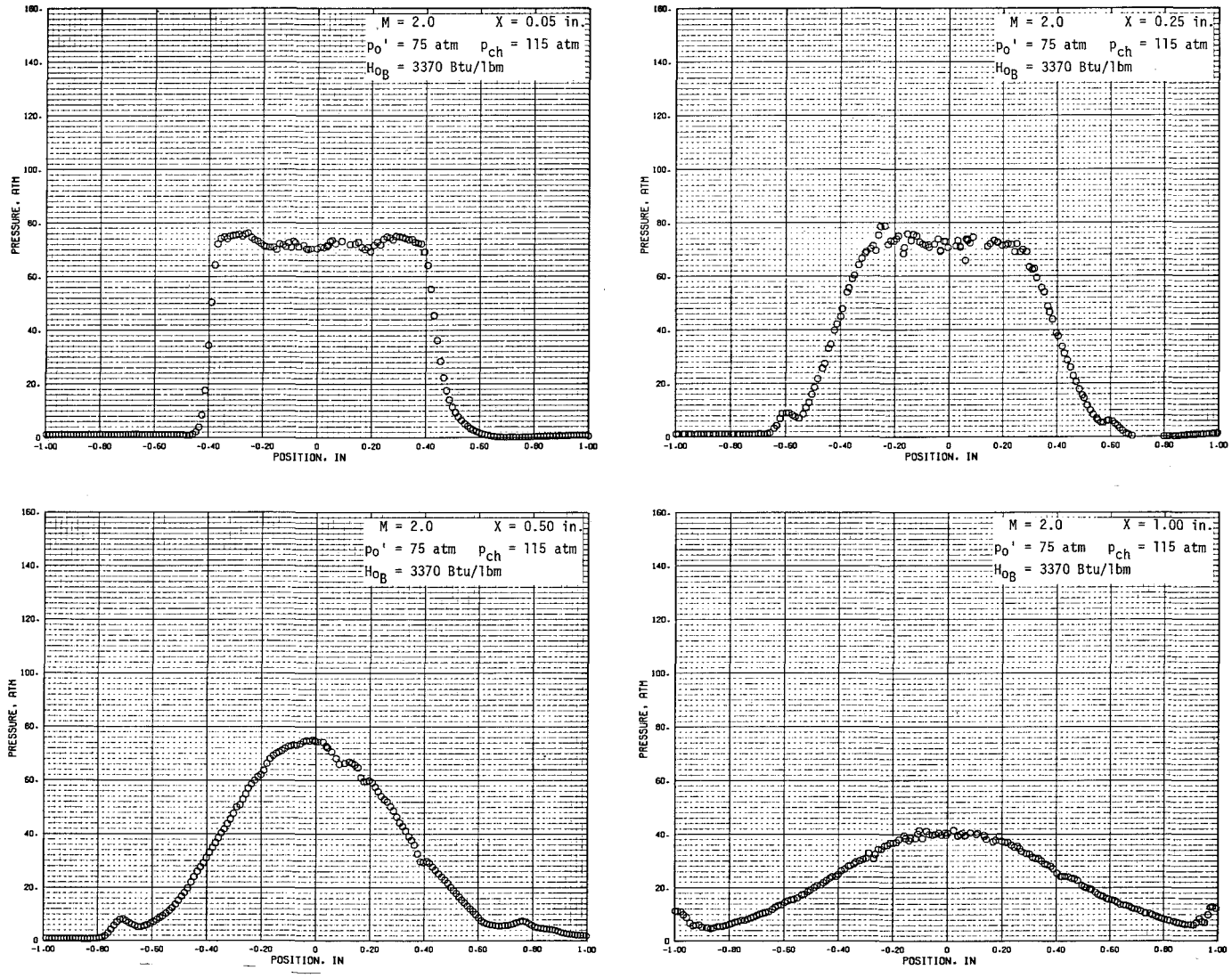

Figure 22. Concluded.

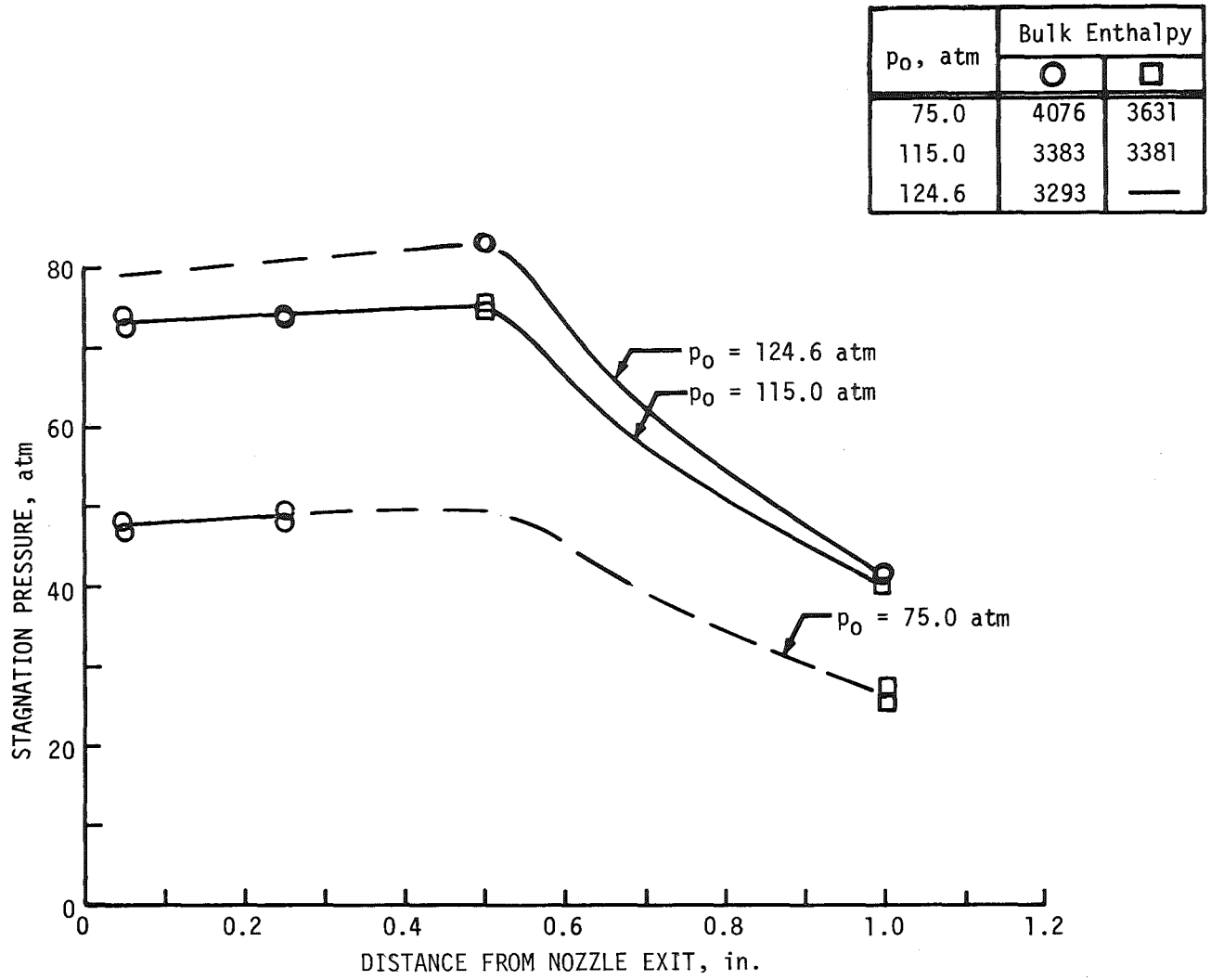

Figure 23. Centerline axial pressure distribution for M = 2.0, d* = 0.625 in., d_e = 0.850 in., and I = 950 amp.

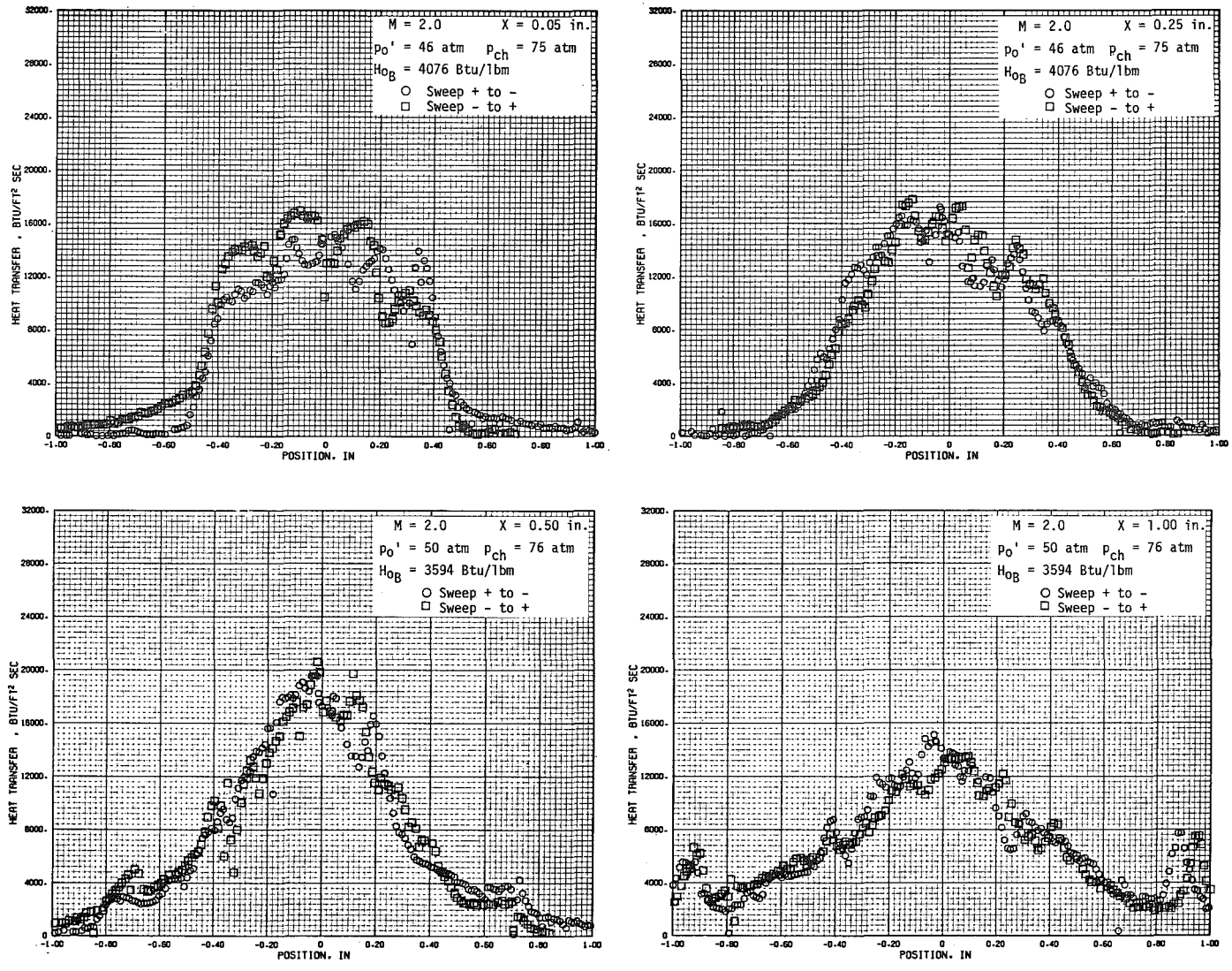

Figure 24. Radial heat-transfer profiles using a calorimeter with R_N = 0.25 in., M = 2.00, d* = 0.625 in., d_e = 0.850 in., and I = 950 amp.

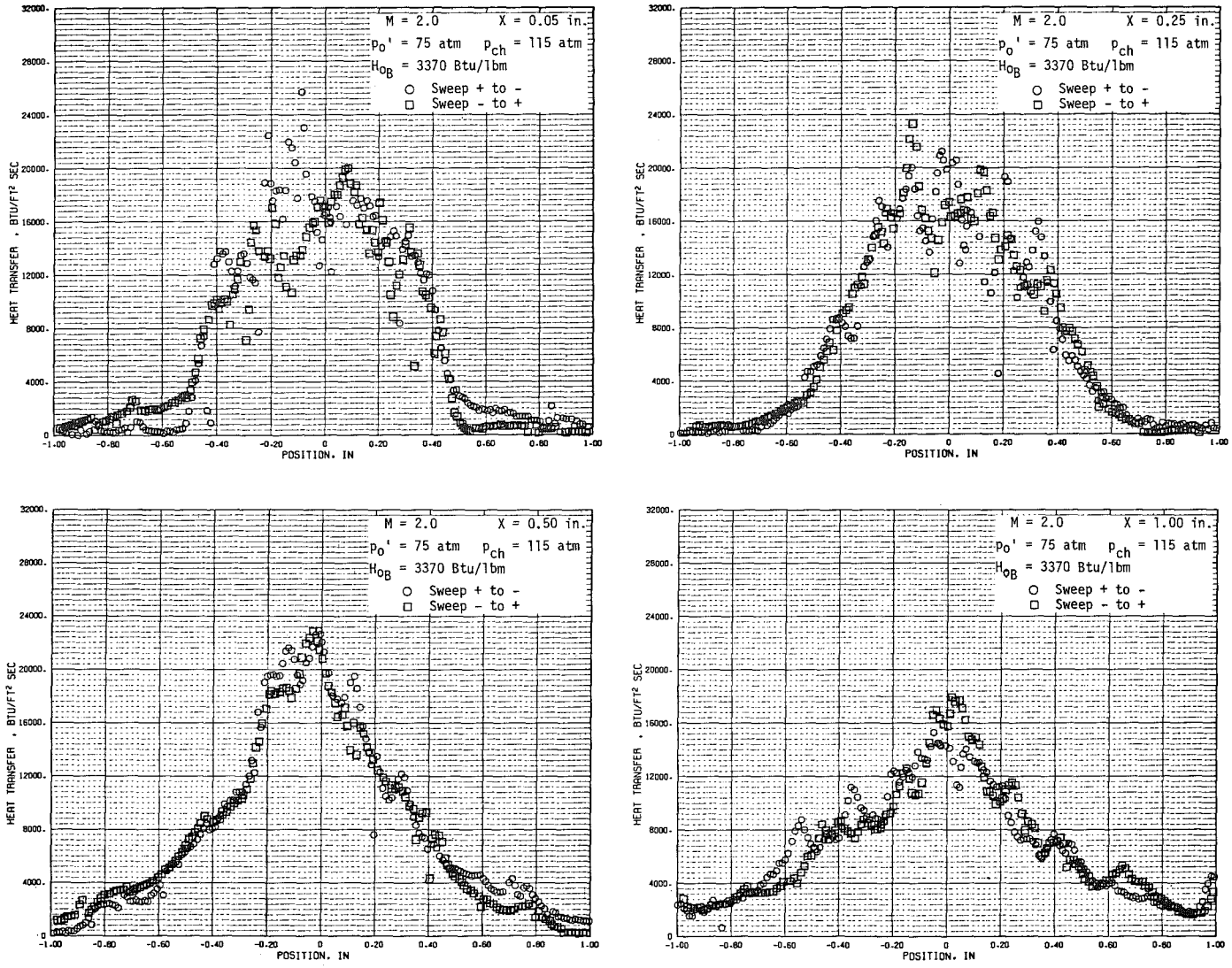

Figure 24. Concluded.

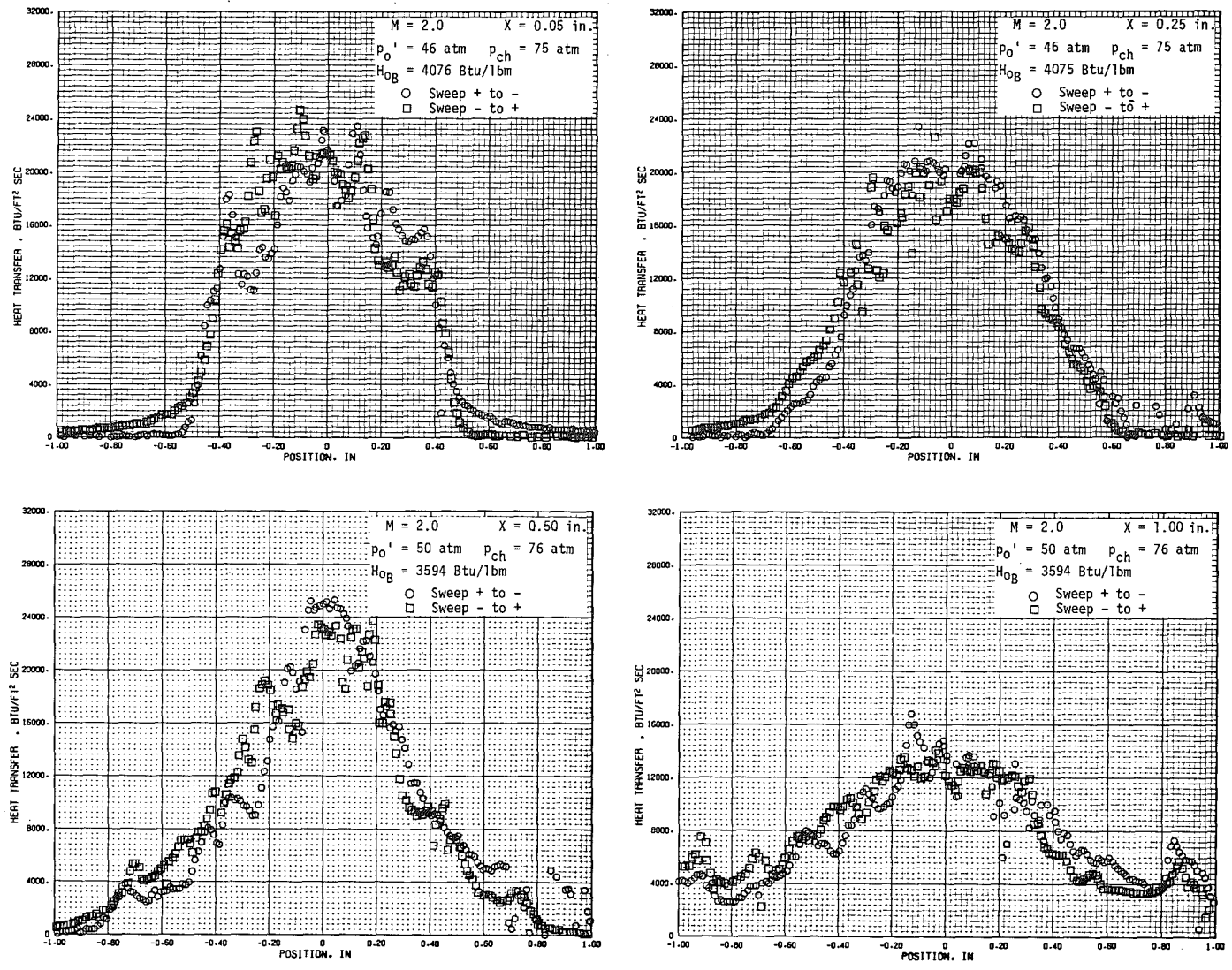

Figure 25. Radial heat-transfer profiles using a calorimeter with R_N = 0.15 in., M = 2.0, d* = 0.625 in., d_e = 0.850 in., and I = 950 amp.

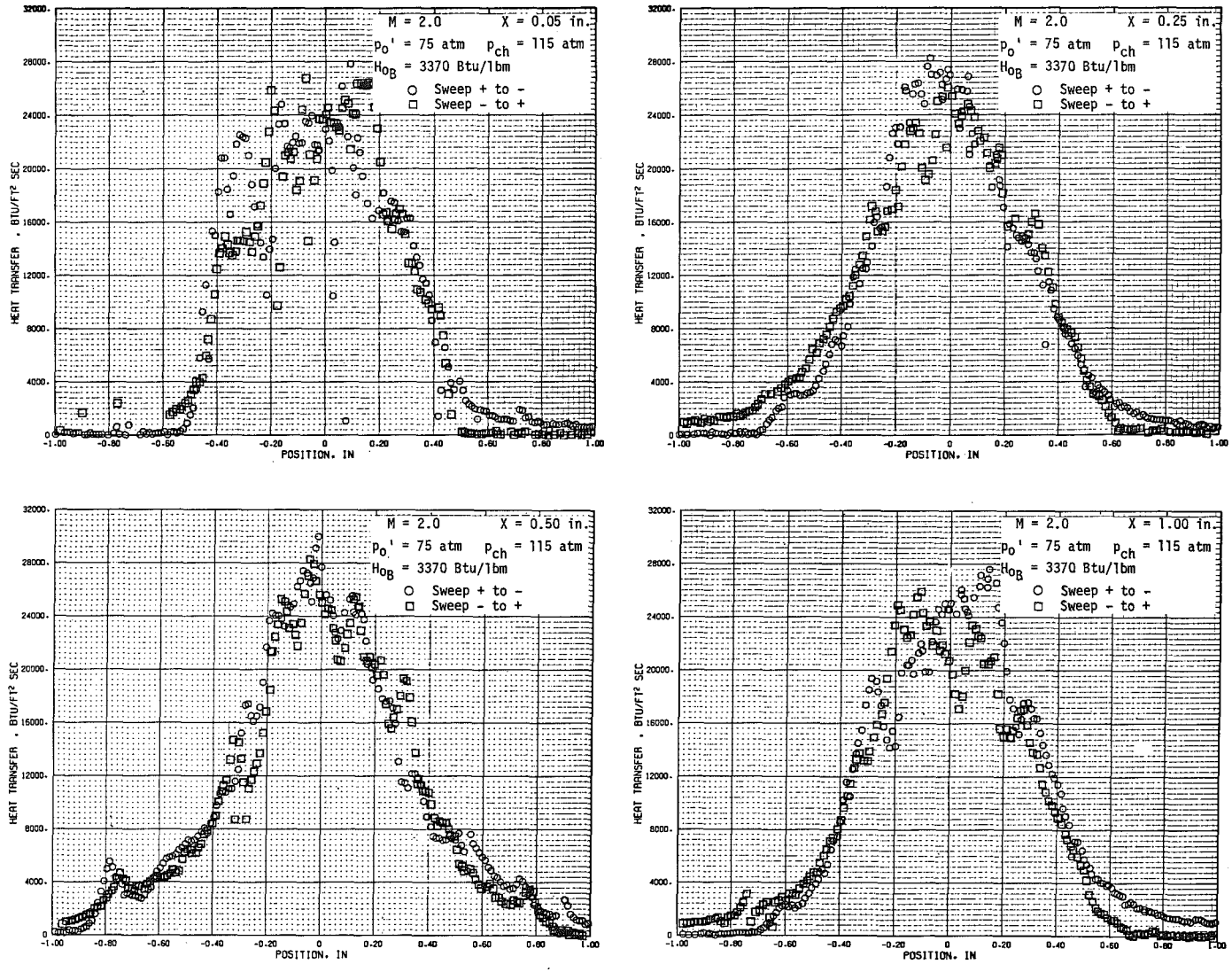

Figure 25. Concluded.

p_o, atm	Enthalpy, Btu/lb	
	○	□
75.0	4076	3626
115.0	3383	3381
124.6	3293	—

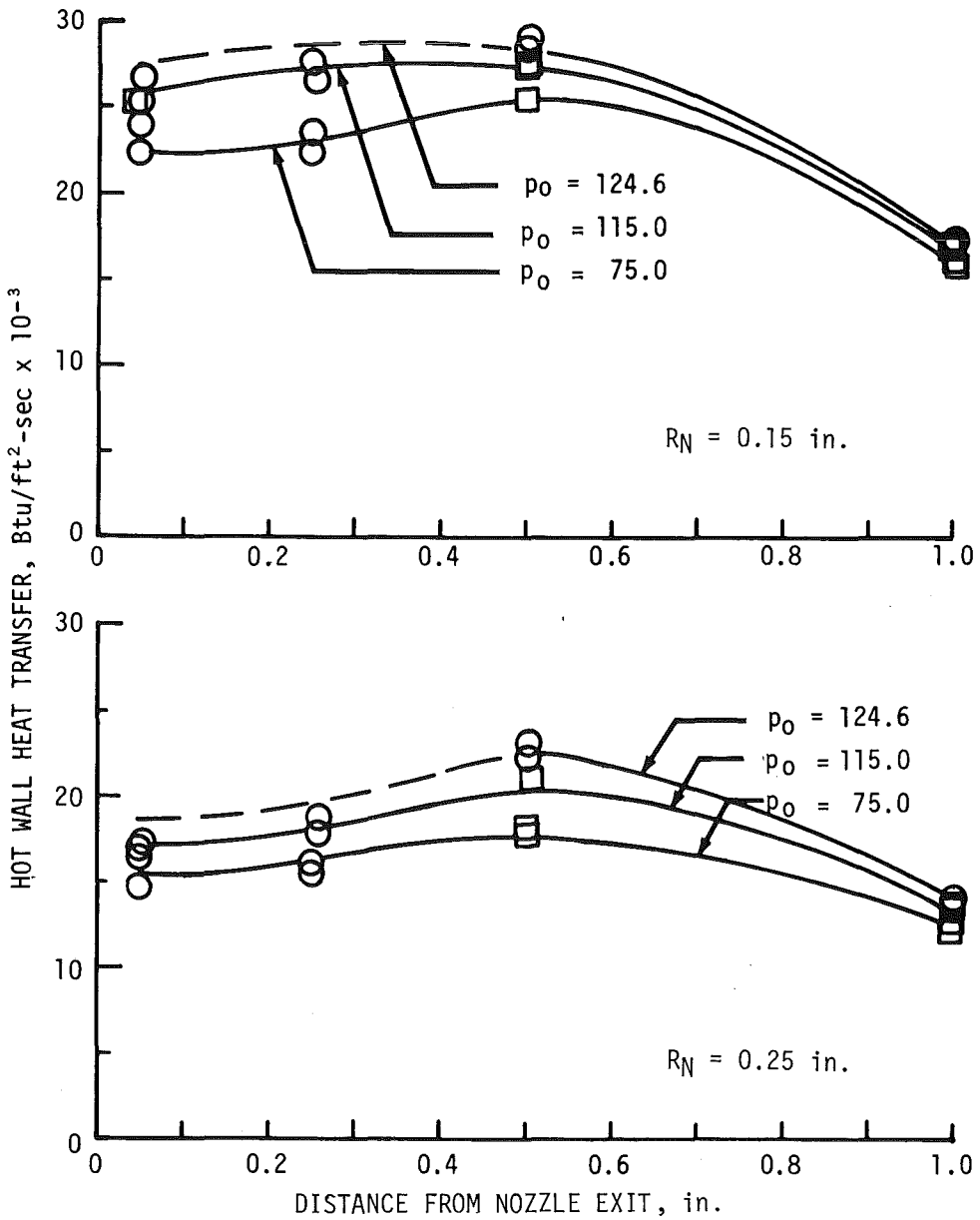

Figure 26. Centerline axial heat-transfer distribution, M = 2.0, d* = 0.625 in., d_e = 0.850 in., and I = 950 amp.

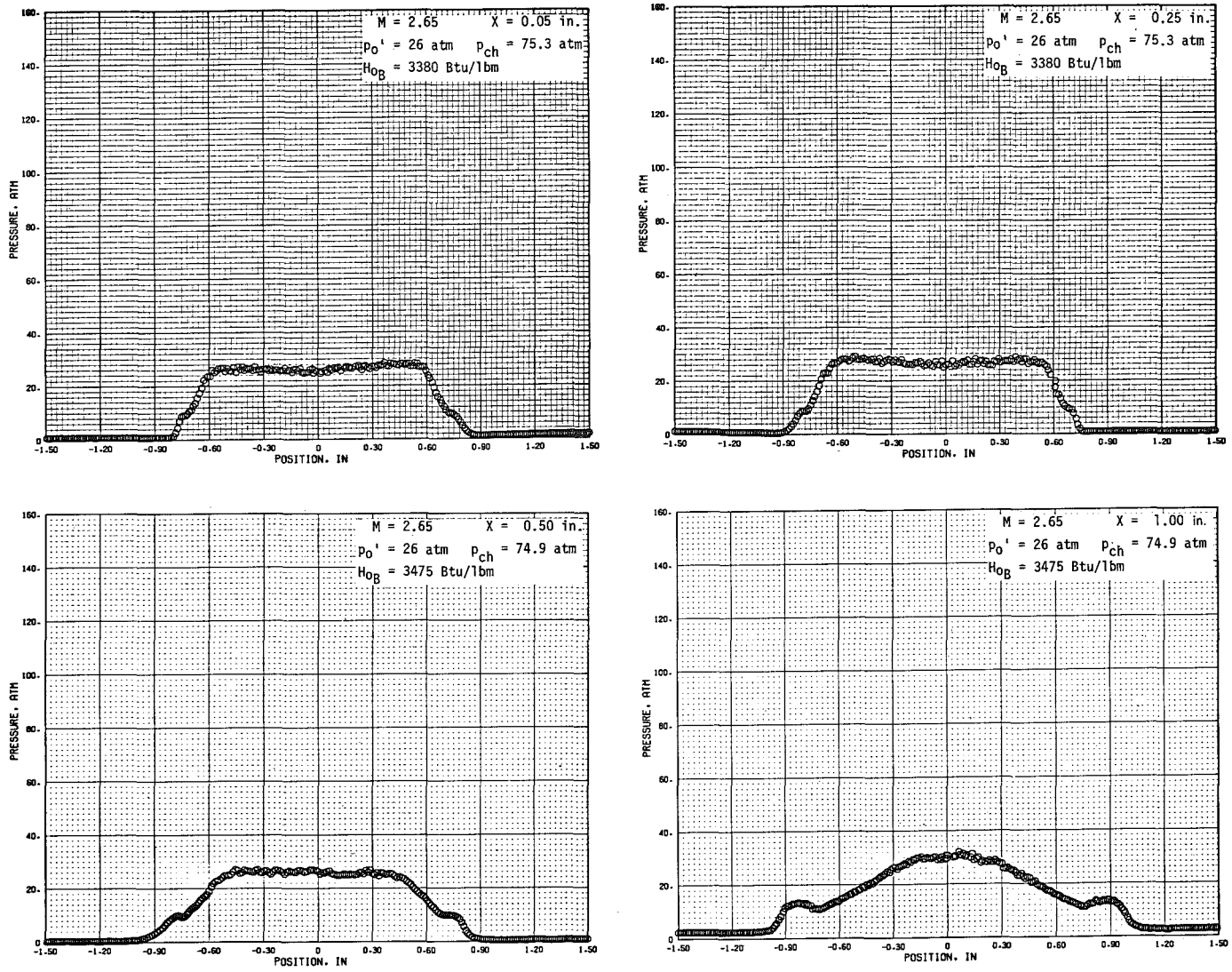

Figure 27. Radial pressure profiles, M = 2.65, d* = 0.700 in., d_e = 1.400 in., and I = 990 amp.

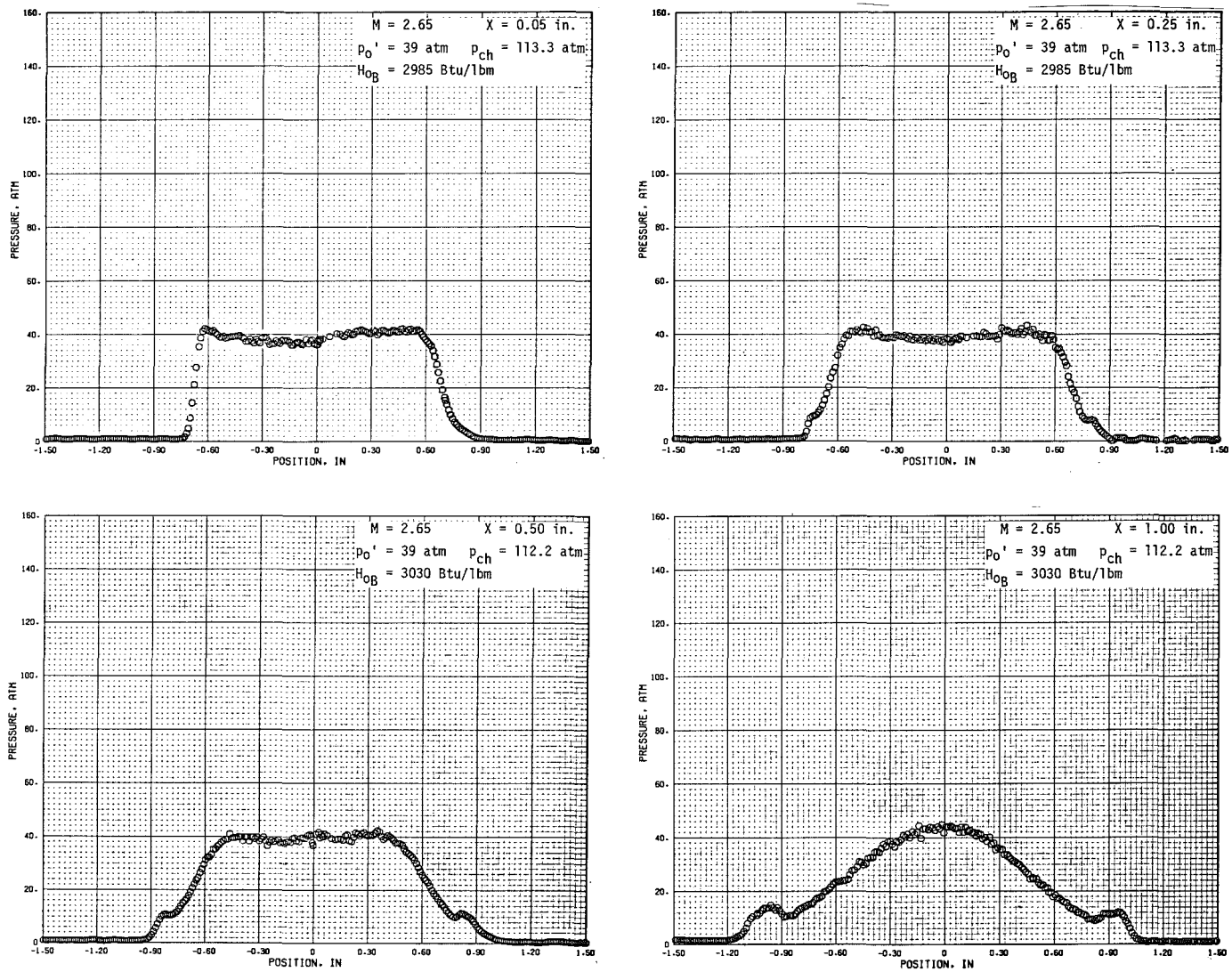

Figure 27. Concluded.

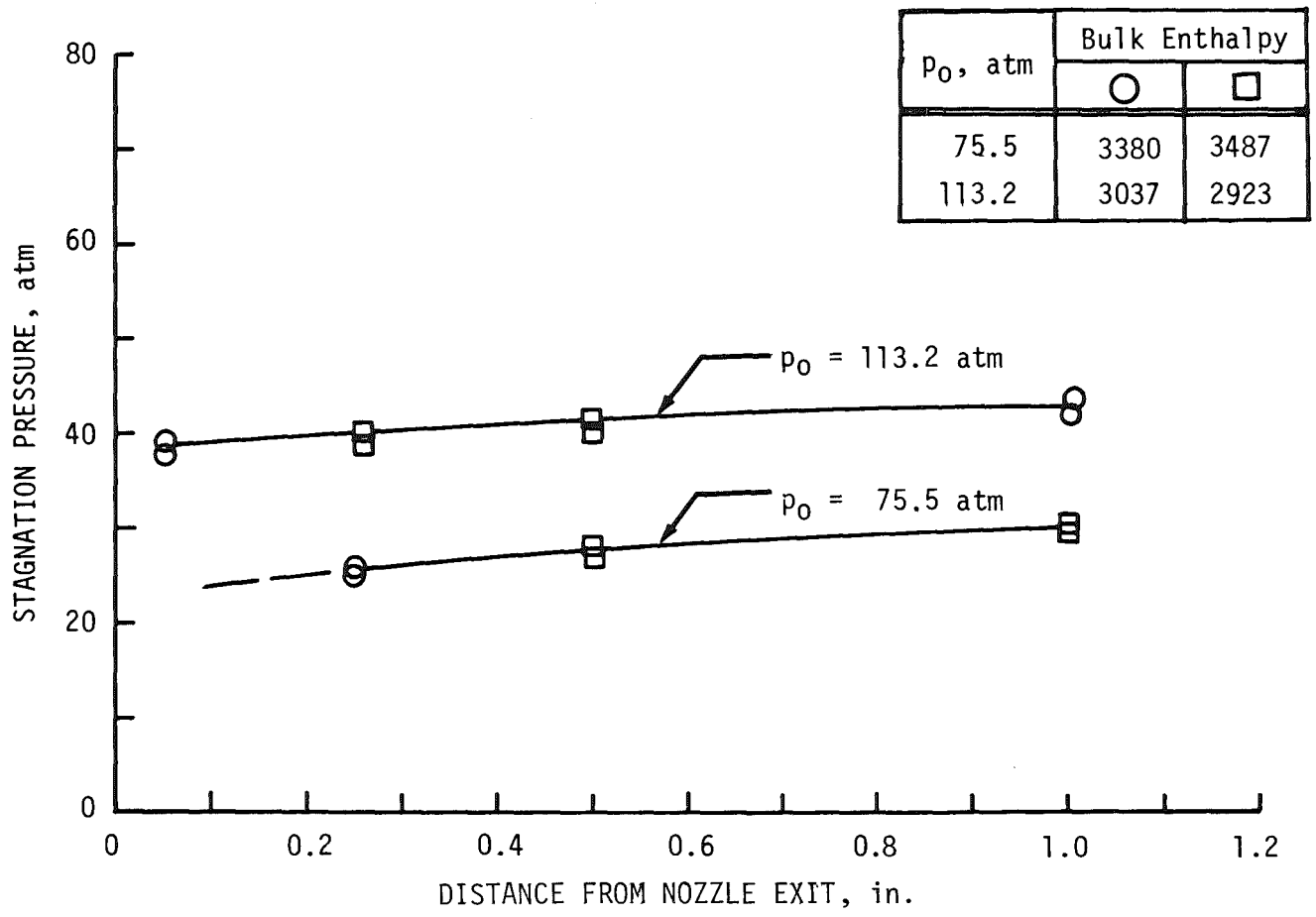

Figure 28. Centerline axial pressure distribution, M = 2.65, d* = 0.700 in., d_e = 1.400 in., and I = 990 amp.

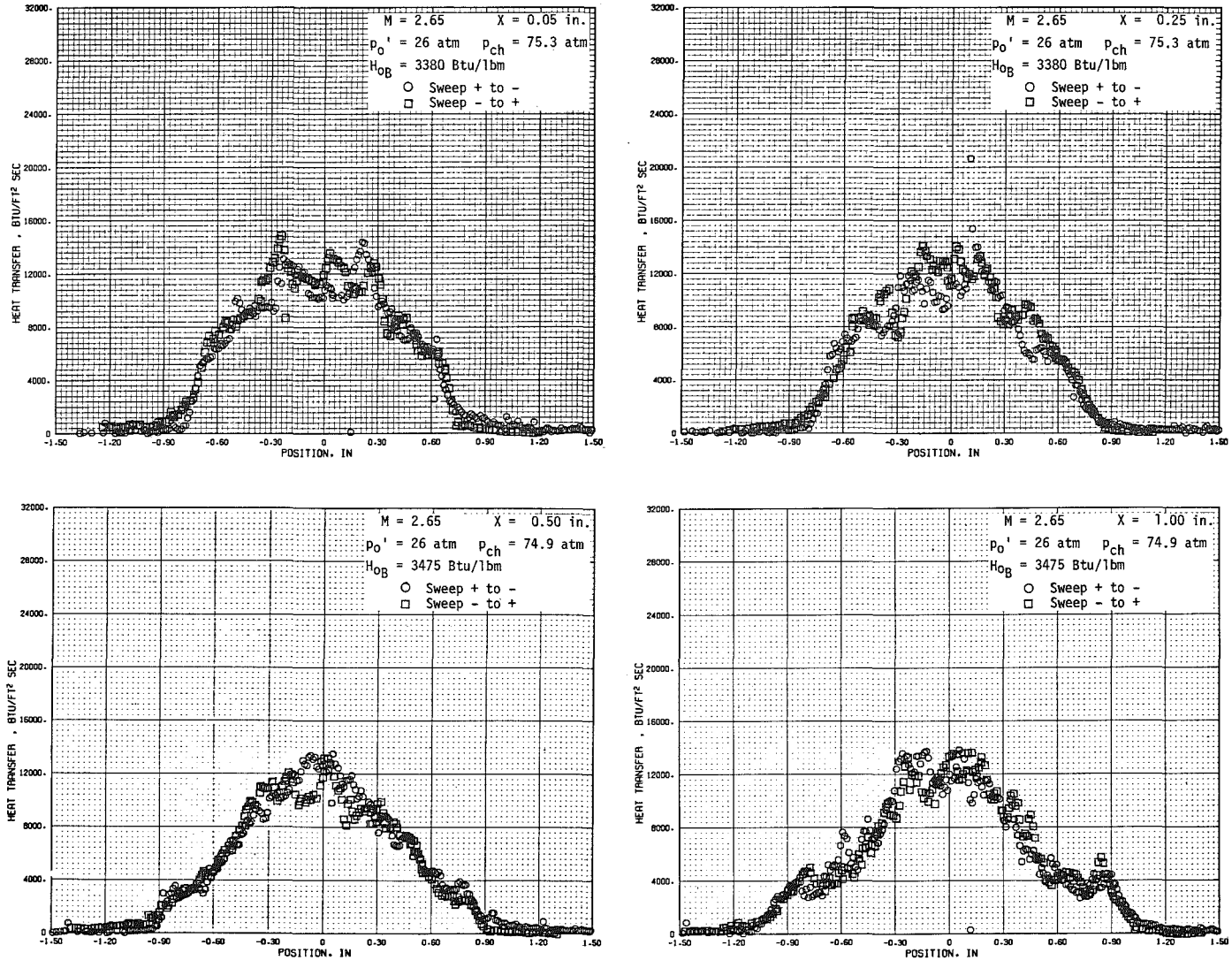

Figure 29. Radial heat-transfer profile using a calorimeter with R_N = 0.25 in., M = 2.65, d* = 0.700 in., d_e = 1.400 in., and I = 990 amp.

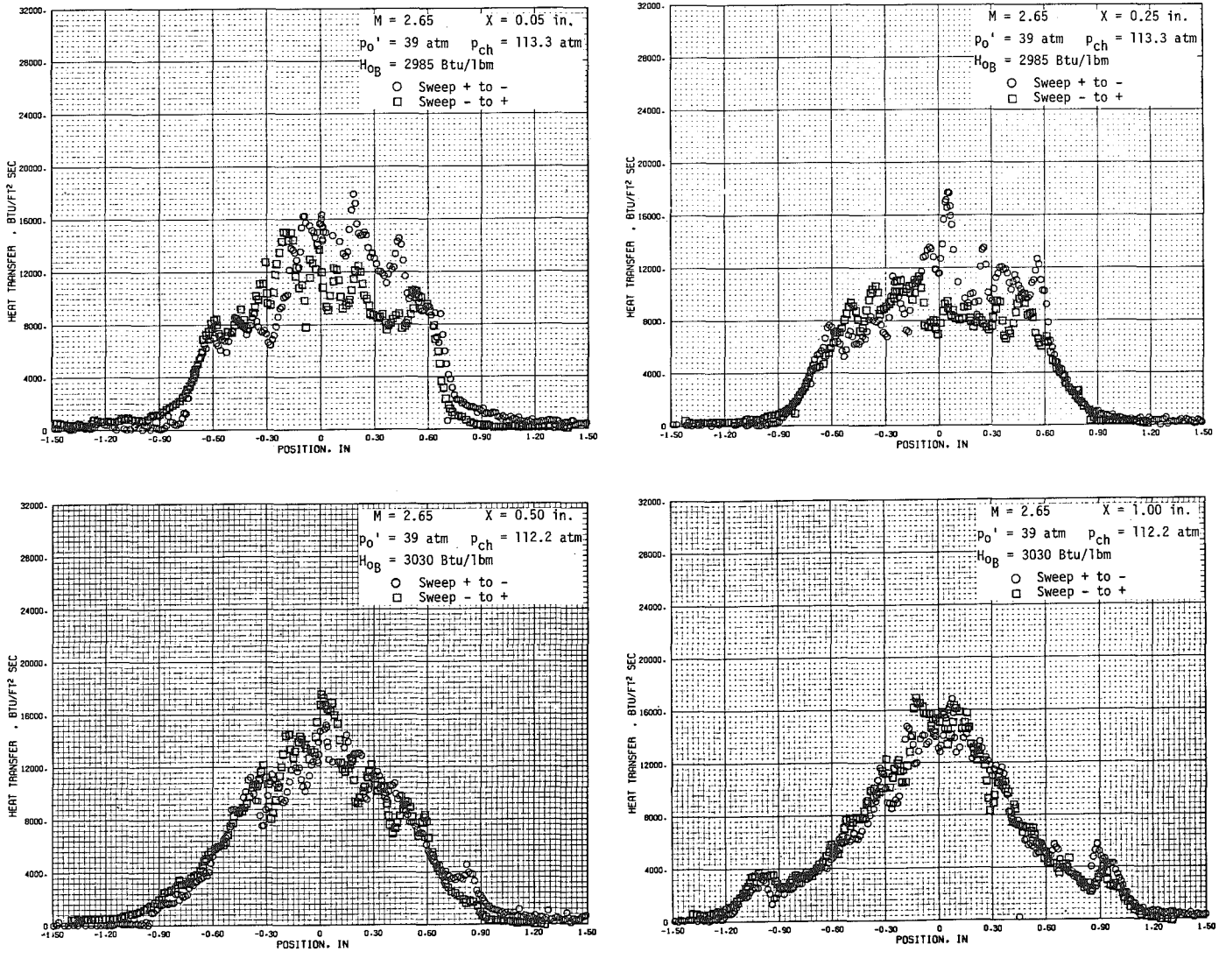

Figure 29. Concluded.

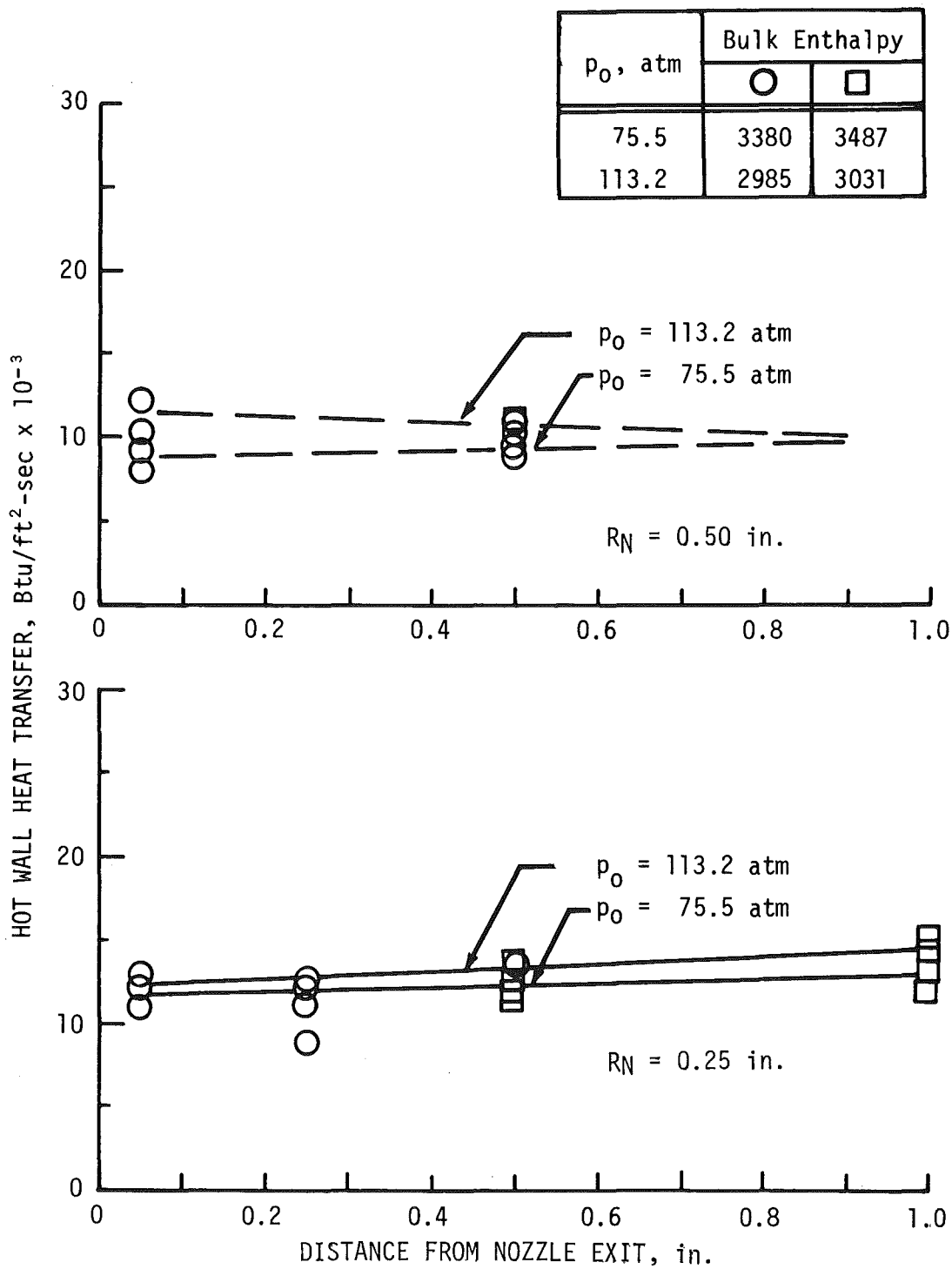

Figure 30. Centerline axial hot wall heat-transfer distribution, M = 2.65, d* = 0.700 in., d_e = 1.400 in., and I = 990 amp.

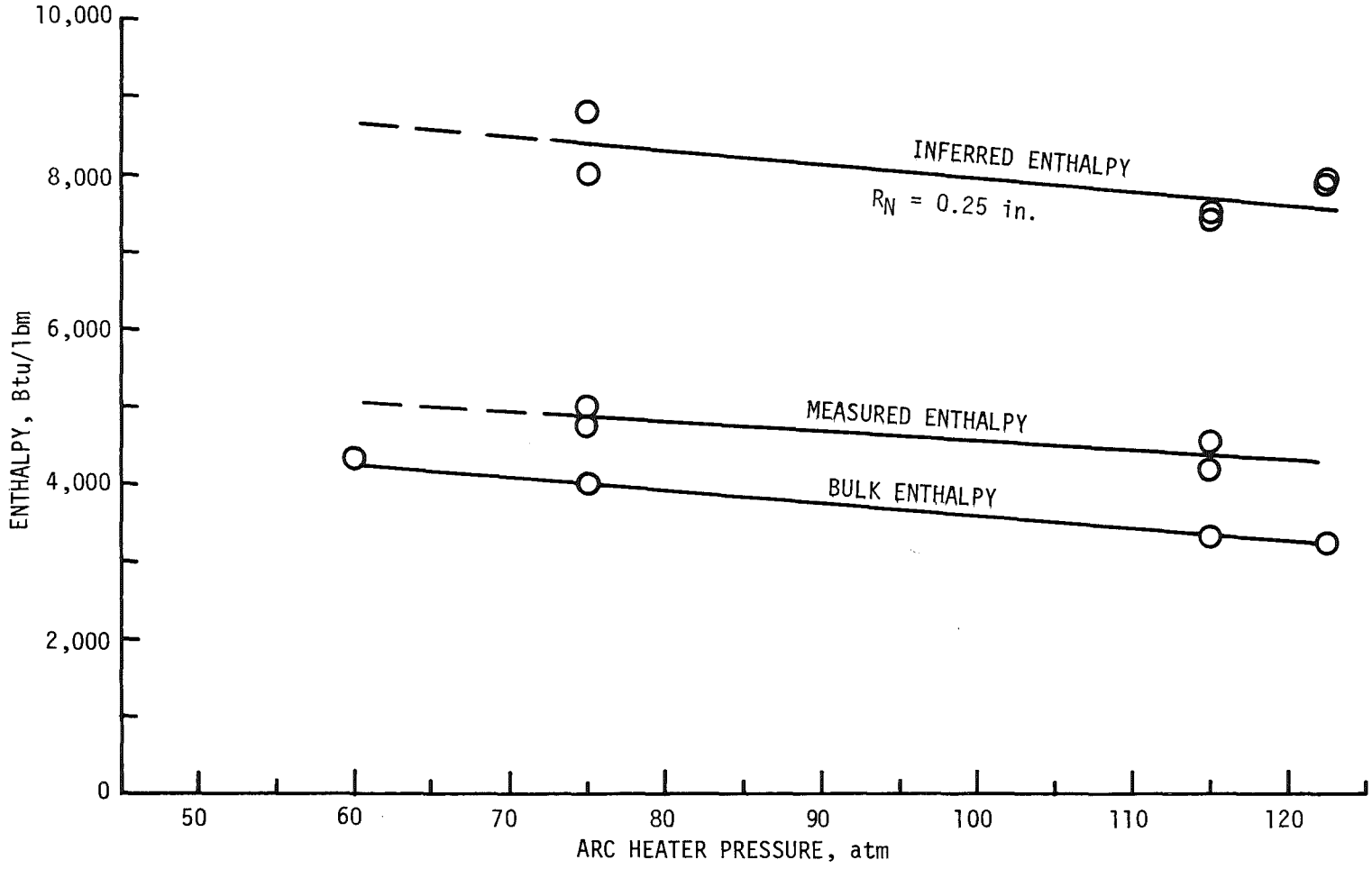

Figure 31. Enthalpy variation with arc heater pressure, M = 2.0, d^* = 0.625 in., d_e = 0.850 in., and I = 950 amp.

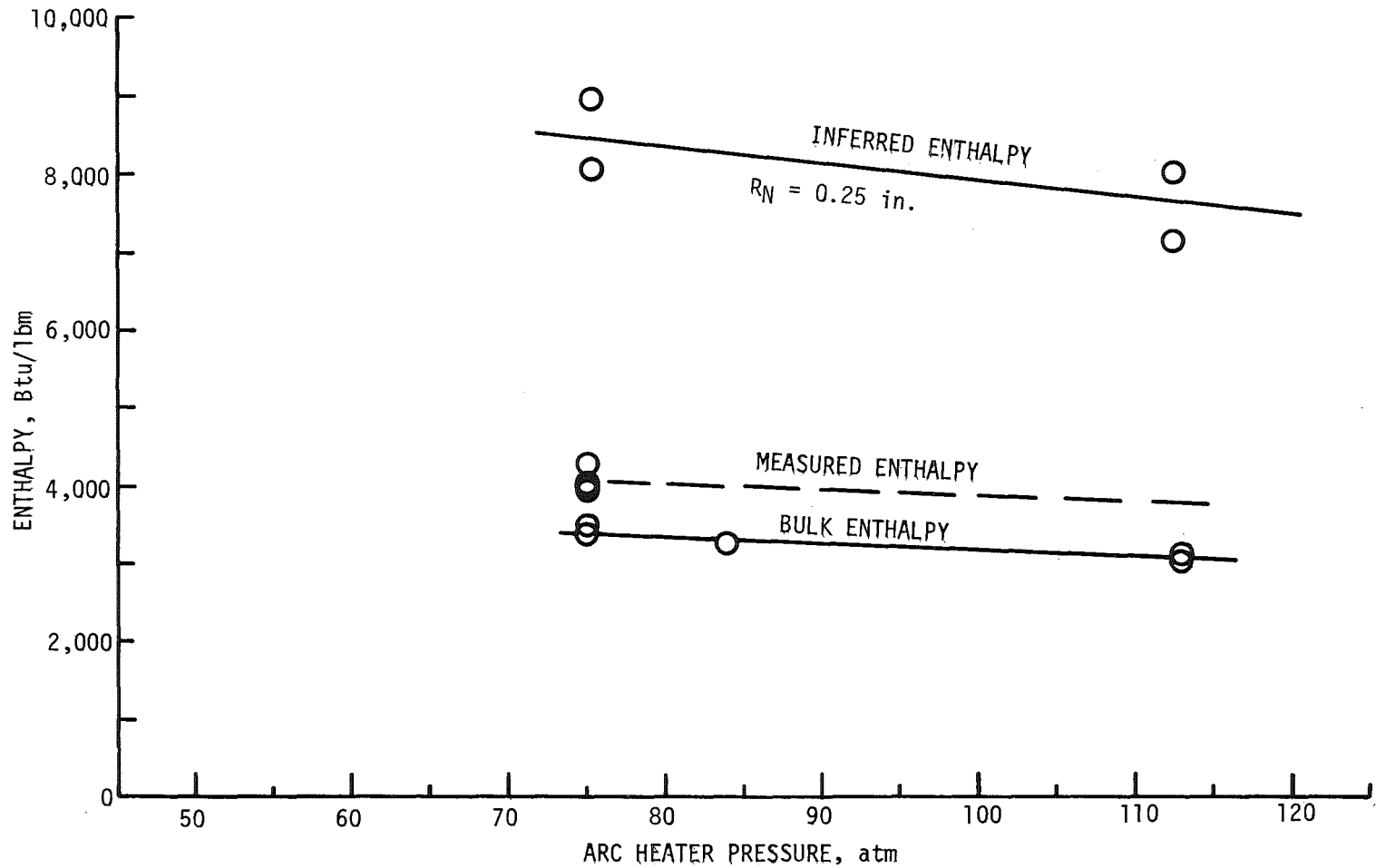

Figure 32. Enthalpy variation with arc heater pressure, M = 2.65, d^* = 0.700 in., d_e = 1.400 in., and I = 990 amp.

Table 1. HEAT (H-1) Available Nozzles

Throat Diameter, in.	Exit Diameter, in.	Exit Mach No.	Model Pressure / Heater Pressure	Type of Nozzle
0.625	0.770	1.80	0.800	Contoured
0.625	0.850	2.00	0.700	Contoured
0.625	0.850	1.80	0.773	Contoured with dust erosion extensions
0.625	1.120	2.50	0.461	Contoured
0.625	1.600	3.00	0.282	Contoured
0.700	1.400	2.65	0.400	Contoured
0.700	1.400	2.52	0.416	Contoured with dust erosion extensions
0.900	1.350	1.80	0.800	Flared

Table 2. Available Photographic Equipment

Camera Type	Manufacturer	Negative Size	Framing Rate, Frames/sec	Film Frames/ft	Magazine Capacity, ft	Number Available	Comments
Motion Picture	Hycam	16 mm	100–10,000	40	400	2	
Motion Picture	Locam	16 mm	50–500	40	400	1	
Motion Picture	Locam	16 mm	50–500	40	400	1	Digital data on each frame
Single Frame	Veriton	70 mm	1	3.4	100	1	Remote control
Motion Picture	Cine Special	16 mm	24–60	40	200	1	Survey coverage
Motion Picture	Milliken	16 mm	100	40	400	1	Survey coverage
Still	Speedgraphic	4x5 in.	Single	—	—	1	
TV	Panasonic	Video Tape	30	71	2,150	2	Slow motion/stop action Split screen

Table 3. Diagnostic Tools Available for Facility Flow Calibration

Flow Diagnostic Type	Direct Measurement	Range	Nose Radius
Impact Pressure Probe	Flow Pressure Profile	5–100 atm	0.040 in.
Heat-Transfer Probe	Stagnation Point Heat Transfer	1,000–30,000 Btu/ft^2-sec	0.250 in.
Transient Enthalpy Probe	Total Enthalpy Profile	500–6,000 Btu/lbm	0.125 in.
Pressure Distribution Probe	7-Channel Pressure Distribution	1–100 atm	0.250 in.
Pressure Distribution Probe	7-Channel Pressure Distribution	1–100 atm	0.500 in.
Heat-Transfer Distribution Probe	7-Channel Heat-Transfer Distribution	200–30,000 Btu/ft^2-sec	0.250 in.
Heat-Transfer Distribution Probe	7-Channel Heat-Transfer Distribution	200–30,000 Btu/ft^2-sec	0.500 in.
Laser Velocimeter	Erosion Particle Velocity	1,000–8,000 ft/sec	---
Pyrometer	Ablating Surface Temperature	2,500–7,500°R	---

Table 4. Run Summary – Large Segmented Arc Heater for Runs > 5 sec through FY77

Run No.	Run Time, sec	d*, in.	p_o, atm	I, amp	V, volts	Power, MW	$\dot{m}$, lb/sec	H_{o_B}, Btu/lb	Efficiency, percent
4–009	5.3	0.625	51	772	11,725	9.1	1.10	4,260	53.5
4–028	5.8	↓	73	696	15,575	10.8	1.80	3,270	55.4
4–019	10.1		71	764	13,400	10.2	1.85	2,900	49.0
4–021	20.7		71	780	13,050	10.2	1.84	2,900	50.0
4–034	6.7		79	670	17,000	11.4	1.85	3,150	52.0
4–035	20.3		76.7	689	16,600	11.4	1.76	3,250	50.8
4–062	10.5		76.8	745	15,642	11.7	1.75	3,415	52.1
4–050	8.8		76.5	780	14,800	11.5	1.80	3,300	52.0
4–074	10.6		73.8	787	14,440	11.4	1.71	3,362	51.7
4–073	10.2		72	790	14,000	11.1	1.66	3,300	50.0
4–051	97.7		72	812	13,680	11.1	1.63	3,230	48.2
4–069	10.4		72	820	13,800	11.3	1.67	3,350	50.0
4–046	7.7		71	840	13,300	11.2	1.65	3,400	50.5
4–098	7.0		76	908	14,400	13.1	1.71	3,650	49.0
4–089	5.7		75	915	14,200	13.0	1.68	3,800	50.0
4–099	20.2		74	916	14,000	12.8	1.64	3,900	51.0
4–090	6.0		73	925	13,900	12.9	1.63	3,850	49.0
6–006	19.3		79	922	14,840	13.7	1.76	3,879	50.9
6–001	18.8		73.4	972	13,600	13.2	1.59	4,136	50.8
4–079	11.4		75.3	1,016	13,740	14.0	1.62	3,935	46.6
4–057	7.9		115	900	18,700	16.8	2.74	3,120	51.5

Table 4
Concluded

Run No.	Run Time, sec	d*, in.	p_o, atm	I, amp	V, volts	Power, MW	$\dot{m}$, lb/sec	H_{o_B}, Btu/lb	Efficiency, percent
4-101	8.2	0.625	110	948	18,200	17.3	2.62	3,140	48.0
4-102	15.6	↓	108	951	18,200	17.3	2.52	3,330	49.0
4-109	20.1	↓	113	965	18,400	17.8	2.63	3,460	52.0
6-003	20.4	↓	115	923	19,190	17.7	2.70	3,401	52.7
6-002	5.7	↓	119	934	19,733	18.4	2.78	3,455	52.9
6-004	19.9	↓	114	955	18,990	18.1	2.64	3,598	53.4
4-112	12.2	↓	115	963	18,800	18.1	2.65	3,440	51.3
4-113	30.5	↓	110	1,000	17,800	17.8	2.53	3,350	48.4
6-012*	28.4	0.625	60.8	1,163	10,868	12.6	1.32	4,277	45.8
			124	926	19,975	18.5	2.93	3,332	53.7
4-116	6.2	0.700	74	977	14,700	14.4	2.12	3,500	53.0
6-007	18.5	↓	74	989	14,630	14.5	2.14	3,516	52.9
6-009	18.9	↓	74	992	14,640	14.5	2.13	3,612	53.8
6-010	18.9	↓	112	979	19,767	19.4	3.44	3,115	56.1
6-013	19.2	↓	115	1,001	19,554	19.6	3.56	2,926	53.8
6-011	18.7	↓	113	1,005	19,553	19.7	3.46	3,034	54.1
4-125	5.2	↓	113	1,010	19,500	19.7	3.48	3,000	54.0

*Ramp Test

NOMENCLATURE

D_p	Particle diameter, microns
d_e	Nozzle exit diameter, in.
d*	Nozzle throat diameter, in.
H_{o_B}	Bulk enthalpy, Btu/lbm
H_s	Sonic flow enthalpy, Btu/lbm
I	Arc current, amp
M	Mach number
p_o	Total pressure, chamber pressure, atm
p_o'	Impact pressure, atm
V	Arc potential, v
x	Distance downstream of nozzle exit, in.
R_N	Model nose radius, in.